



Piezoelectric polymer wind generators
by Hadi Darejeh

A thesis submitted in partial fulfillment of the requirements for the degree of Master of Science in
Physics

Montana State University

© Copyright by Hadi Darejeh (1983)

Abstract:

Small wind generators based on the piezoelectric effect in poly(vinylidene fluoride), or PVF2 for short were designed, built and tested. The design was based on developing a voltage across a bimorph made of two PVF2 sheets glued back-to-back and coated with electrodes. Suitable means of setting these bimorphs into oscillation in the wind were developed. One of these designs (oscillating leaf) is based on forcing the blades into oscillation at 60 Hz and feeding the output directly into the ac line. The other two designs had the blades as parts of rotors which were forced to rotate by the wind. For these designs the power was brought out through the rotor bearings and could be fed into the line by means of a rectifier and synchronous inverter. The poled PVF2 is very expensive, but reducing the cost of the poling process could make PVF2 wind generators practical for commercial use.

PIEZOELECTRIC POLYMER WIND GENERATORS

by

Hadi Darejeh

A thesis submitted in partial fulfillment
of the requirements for the degree

of

Master of Science

in

Physics

MONTANA STATE UNIVERSITY
Bozeman, Montana

December 1983

MAIN LIB.
N378
D245
cop. 2

APPROVAL

of a thesis submitted by

Hadi Darejeh

This thesis has been read by each member of the thesis committee and has been found to be satisfactory regarding content, English usage, format, citations, bibliographic style, and consistency, and is ready for submission to the College of Graduate Studies.

Dec. 20, 1983
Date

V. Hugo Schmidt
Chairperson, Graduate Committee

Approved for the Major Department

Dec. 20, 1983
Date

W. J. Swann
Head, Major Department

Approved for the College of Graduate Studies

29 Dec. 1983
Date

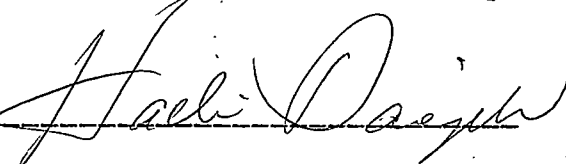
Michael Malone
Graduate Dean

STATEMENT OF PERMISSION TO USE

In presenting this thesis in partial fulfillment of the requirements for a master's degree at Montana State University, I agree that the Library shall make it available to borrowers under rules of the Library. Brief quotations from this thesis are allowable without special permission, provided that accurate acknowledgment of source is made.

Permission for extensive quotation from or reproduction of this thesis may be granted by my major professor, or in his/her absence, by the Director of Libraries when, in the opinion of either, the proposed use of the material is for scholarly purposes. Any copying or use of the material in this thesis for financial gain shall not be allowed without my written permission.

Signature



Date

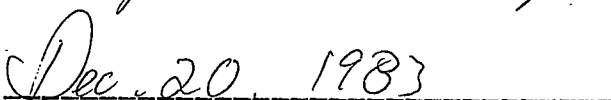


TABLE OF CONTENTS

	Page
LIST OF FIGURES.....	v
ABSTRACT.....	vii
1. INTRODUCTION.....	1
2. THEORY.....	5
3. PROCEDURE.....	24
4. CONCLUSION.....	55
REFERENCES.....	58
APPENDICES.....	60
Appendix I - Figures, Graphs and Datas.....	61
Appendix II - Figures and Plots.....	68
Appendix III - Energy Analysis Calculation.....	74

LIST OF FIGURES

	Page
Figure 1: Electromechanical coupling in piezo- electrics.....	5
Figure 2: An applied force produces electric polari- zation in piezoelectric solids.....	6
Figure 3: Dimensional changes of a piezoelectric solid in an external field.....	7
Figure 4: (a) Piezoelectric material. (b) An electric field induces dimensional expansion. (c) Reverse polarity produces a contraction.	8
Figure 5: (a) tg^+tg^- (b) all trans.....	10
Figure 6: Schematic representation of making piezo- electric film.....	11
Figure 7: Blade tip shape.....	13
Figure 8: Geometry of deflection angle.....	16
Figure 9: Cantilever blade.....	18
Figure 10: Cantilever torque analysis.....	18
Figure 11: Frequency <u>vs.</u> amplitude response.....	21
Figure 12: Circuit to measure Y, d_{ij}	24
Figure 13: Geometry of blade root.....	28
Figure 14: Capacitive blade generator.....	32
Figure 15: Blade as current generator.....	33
Figure 16: Blade as voltage generator.....	33
Figure 17: RLC representation of generator.....	34
Figure 18: Impedance matching circuit for the generator power output.....	35
Figure 19: Power <u>vs.</u> load resistance curves.....	37

LIST OF FIGURES (continued)

	Page
Figure 20: Savonius rotor design for oscillating blades.....	38
Figure 21: Top view cross section of Savonius rotor with PVF ₂ bimorph.....	40
Figure 22: Plot of power <u>vs.</u> load resistance of S-rotor generator.....	41
Figure 23: Cross section of oscillator leaf.....	44
Figure 24: Front view of an oscillator leaf.....	44
Figure 25: Output power <u>vs.</u> load resistance for oscillating leaf.....	45
Figure 26: Circuit representation of three generators in parallel.....	51
Figure 27: Equivalent circuit of figure 26.....	52
Figure 28: Y and d _{ij} measurement apparatus.....	62
Figure 29: Stress-strain curve.....	63
Figure 30: Load <u>vs.</u> voltage drop graph for d ₃₁	64
Figure 31: Load <u>vs.</u> voltage drop graph for d ₃₂	65
Figure 32: Circuit diagram for determining Q and f _r ...	66
Figure 33: Plot of frequency <u>vs.</u> amplitude for Q and f _r determination.....	67
Figure 34: Plot of α <u>vs.</u> ω	69
Figure 35: Lateral leaf rotor construction figure...	70

ABSTRACT

Small wind generators based on the piezoelectric effect in poly(vinylidene fluoride), or PVF₂ for short were designed, built and tested. The design was based on developing a voltage across a bimorph made of two PVF₂ sheets glued back-to-back and coated with electrodes. Suitable means of setting these bimorphs into oscillation in the wind were developed. One of these designs (oscillating leaf) is based on forcing the blades into oscillation at 60 Hz and feeding the output directly into the ac line. The other two designs had the blades as parts of rotors which were forced to rotate by the wind. For these designs the power was brought out through the rotor bearings and could be fed into the line by means of a rectifier and synchronous inverter. The poled PVF₂ is very expensive, but reducing the cost of the poling process could make PVF₂ wind generators practical for commercial use.

CHAPTER 1

INTRODUCTION

When Coulomb stated the well-known law of the force between two charges, it was thought that electricity could be produced by pressure. First Hauy and then A. C. Becquerel conducted experiments in which particular crystals showed electrical effects when pressure was applied.

Credit should also be given to the brothers Pierre and Jacques Curie for the discovery in 1880 that some crystals when compressed in particular directions produce positive and negative charges on certain portions of their surfaces, these charges being proportional to the pressure, and which then vanish when the pressure is removed.

This wasn't just a lucky discovery, because Pierre Curie's previous study of pyroelectric phenomena led both of them to look for electricity from pressure. They also looked for a particular direction of applying the force and studied which groups of crystals exhibit the effect. So the name piezoelectric, which means electricity by pressure, was given to this class of material.

One of these piezoelectric materials is a

piezoelectric polymer, namely poly(vinylidene fluoride), abbreviated PVDF or PVF₂. The piezoelectric effect in PVF₂ was first discovered by Kawai, a Japanese scientist, in 1969. As the name implies, this phenomenon is an electric polarization of the polymer (solid) on which forces are acting. For reasonable forces the polarization is proportional to the applied force. If the external force is reversed in sign the polarization changes direction. An inverse effect is a dimensional change (a strain) caused by applying an electric field.

PVF₂ and some of its copolymers have been shown to be ferroelectric, while other piezoelectric polymers are less likely to be. PVF₂, whose molecular chain formula is (CH₂-CF₂)_n, appears to be the strongest of piezoelectric and pyroelectric polymers.

In order to make these polymers macroscopically polar, there has to be mechanical extension and electrical poling. Mechanical extension causes a reorientation of the original spherulitic structure into an array of crystallites which now has its molecules oriented in the direction of the force. Now the final step consists of evaporating electrodes on the sample and connecting them to a high voltage source, applying a field of 0.5 megavolt per centimeter. This step creates a permanent polar film.

Wind generator application of PVF_2 , which is the main aspect of this project, is explored herein in great detail. Today wind power can be used to provide electricity by conventional windmills, but a piezoelectric wind generator is quite a different technique to produce this electricity.

If a piezoelectric polymer is set into oscillation by means of wind, the strain in the polymer creates a voltage and since the polymer is oscillating the voltage output will be alternating. Suitable means of setting these polymers into oscillation are developed through three different types of generators. They are named lateral leaf rotor, Savonius rotor, and oscillating leaf. Their engineering aspects are dealt with mainly in the Theory and Procedure sections.

The reason for the design of the lateral leaf rotor is to have as large a rotor as possible consistent with the requirement of 60 Hz blade oscillation frequency so that its 60 Hz power output can be fed into the utility line.

The Savonius (S-cross-section) vertical axis rotor has a low tip speed ratio, but its design shape is very suitable for oscillating blades. This has a flexible blade root made of PVF_2 attached to a central rod which holds the entire assembly together.

For both of these designs the output current from the rotor is taken out through the rotor bearings and fed into a resistor as a test load, with an oscilloscope measuring the voltage created due to the strain in the bimorph blade.

The oscillating leaf generator sets a PVF_2 bimorph blade into oscillating bending motion, thereby creating an ac voltage. A cantilever mounted thin spring steel bar has a PVF_2 blade mounted on the free end. That puts the entire system into oscillation if bar and blade have the same resonant frequency. The blade consists of two sheets of the piezoelectric polymer PVF_2 glued back-to-back onto an inert plastic central layer. The bending alternately causes one PVF_2 sheet to be in tension and the other one in compression, producing a net electric field in the same direction in both sheets for one half cycle, while both fields reverse in the next half cycle.

CHAPTER 2

THEORY

Piezoelectric crystals do not have a center of symmetry. If they have net dipole moments in their unit cells piezoelectrics are also pyroelectrics. However, not all piezoelectric unit cells have net dipoles and therefore not all piezoelectrics are pyroelectrics, Piezoelectricity is produced when a suitable crystal is subjected to mechanical stress. Conversely, if the surfaces of the crystal are electroded and an electric field is applied, deformation of the crystal will result. Some of the electromechanical coupling effects are shown in figure 1.

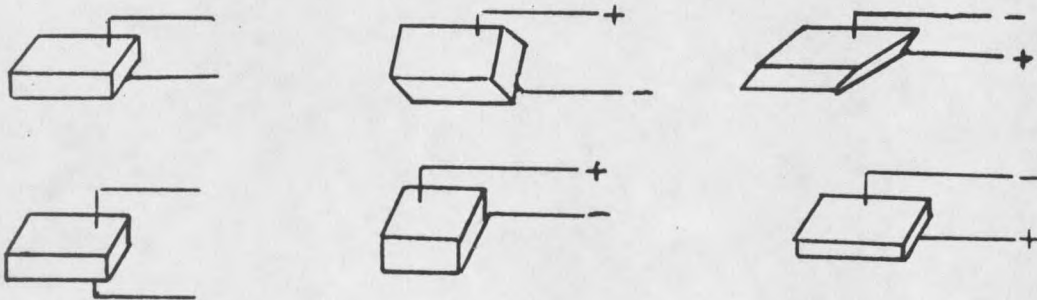


Figure 1. Electromechanical coupling in piezoelectrics.

As the name implies, this phenomenon is a polarization of a solid on which forces are acting (figure 2). For reasonable forces, the amount of polarization is proportional to the magnitude of the applied stress. If the external force is changed in direction, the polarization changes direction accordingly.

The relationship between P and F can be expressed (for a simple geometric figure) as $P = \text{constant} * F$.

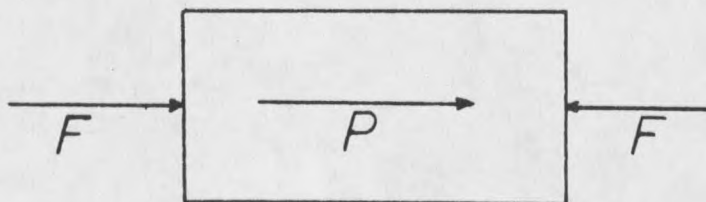


Figure 2. An applied force produces electric polarization in piezoelectric solids. This polarization is shown here collinear with F . In general, P can make any angle with F .

The inverse piezoelectric effect exists also. That is, a dimensional change (a strain) is produced in a crystal when it is placed in an electric field. The inverse piezoelectric effect however is a linear function of the first power of the applied field (for appreciable fields). Therefore the magnitude of the piezoelectric strain S_x in a specimen placed in an electric field E for

a simple shape specimen is given by the relationship $S_x = \text{constant} * E$.

The geometry of the above relation is shown in figure 3. With initial length (no field present) represented by l and the length in the field by $l + \Delta l$, then the strain is $S_x = \Delta l / l$. The inverse effect is sensitive to the direction of the applied field. If the field is reversed, the strain is a contraction.

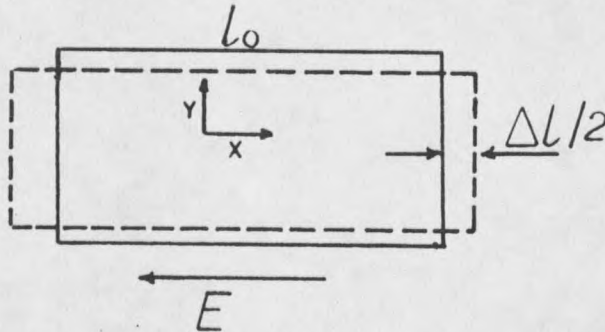


Figure 3. Dimensional changes of a piezoelectric solid in an external field.

A description of what truly happens in the case of applying a field to the polymer is shown in figure 4. This figure also shows the reason for generation of a sound wave.

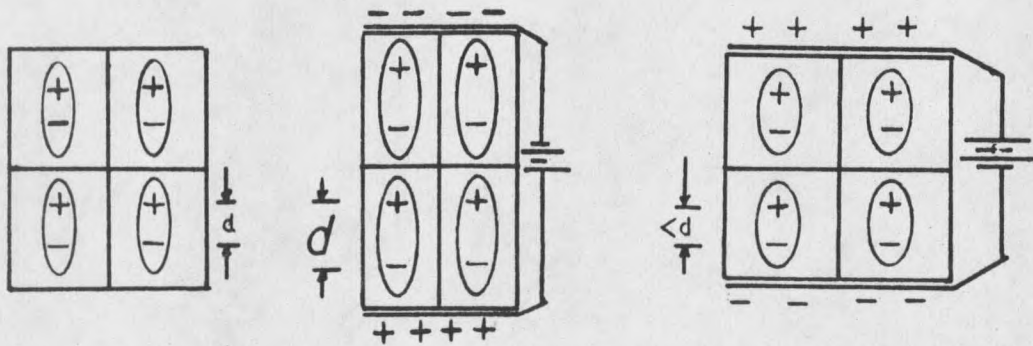


Figure 4. (a) Piezoelectric material. (b) An electric field induces dimensional expansion. (c) Reverse polarity produces a contraction.

The figure of merit for piezoelectrics K is called the coefficient of electromechanical coupling, or

$$K^2 = \frac{\text{Electrical Energy out}}{\text{Mechanical Energy in}} = \frac{\text{Mechanical Energy out}}{\text{Elect Energy in}}$$

K is also related to the dielectric constant ϵ in the following manner.

$$\epsilon_{\text{free}}(1-K^2) = \epsilon_{\text{clamped}}$$

where ϵ_{free} is dielectric constant at low frequency and the clamped dielectric constant is measured at high frequency where the device is effectively clamped by its own inertia. From the mechanical point of view K is also related to Young's Modulus Y , such that:

$$Y_{\text{open ckt}}(1-K^2) = Y_{\text{closed ckt}}$$

The value of Y is measured with closed circuit and with electroded surfaces connected to each other. When shorted the value of Y is less than that for an open

circuit.

Let's consider that there is a single crystal with the dipoles of the unit cells aligned as shown in figure 4. In applying an electric field as exhibited, the crystal lengthens because the ions are attracted to the pole plates. If an AC voltage is applied, the crystal expands and contracts in oscillation, sending out a wave into the surrounding medium, whether air or water. If we apply a mechanical force, the charges shown above build up on the surface, creating a voltage which dies off exponentially when the force is removed. One of the most responsive piezoelectric polymers is poly(vinylidene fluoride), PVF_2 , with the chemical formula $(CH_2-CF_2)_n$.

A few words on the chemical composition of PVF_2 would probably be useful in understanding the piezoelectricity of this material. Macromolecular chains have many elementary repeating unit cells, called monomers, that are linked chemically during polymerization. These monomers have polar chemical groups. To obtain good piezoelectric polymers, their constituents should not be so big that they prevent crystallization of the macromolecules or make them have helical shapes which produce internal gathering of polarization. These macromolecules should also be chemically stable and not cross-linked into infusible and

insoluble solids. Because of the above considerations, fluorocarbons are the best monomers to yield piezoelectric polymer crystals. A schematic representation of the two most common crystalline chains is shown in figure 5.

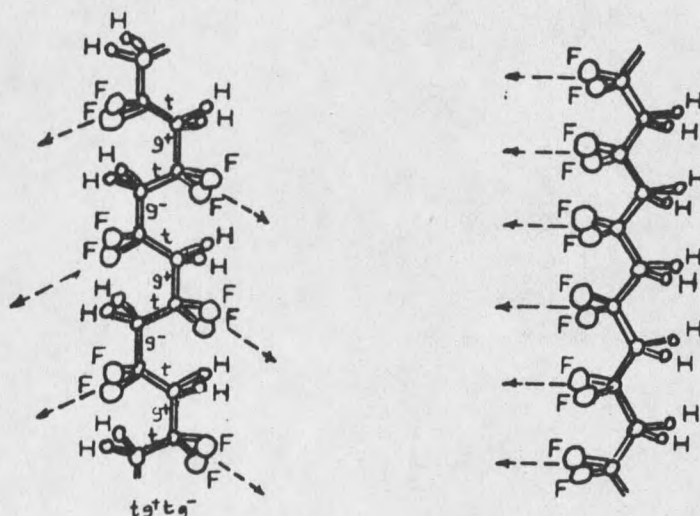


Figure 5. (a) $tg^+ tg^-$ (b) (all trans). The arrows indicate projections of the $-CF_2$ dipole directions on planes defined by the carbon backbone.

The tg^+tg^- configuration has its dipole moments both parallel and perpendicular to the chain axis, while the other one has its dipole moments perpendicular to the molecular axis.

The process by which piezoelectric films are obtained, mentioned on page 2, is shown schematically in figure 6.

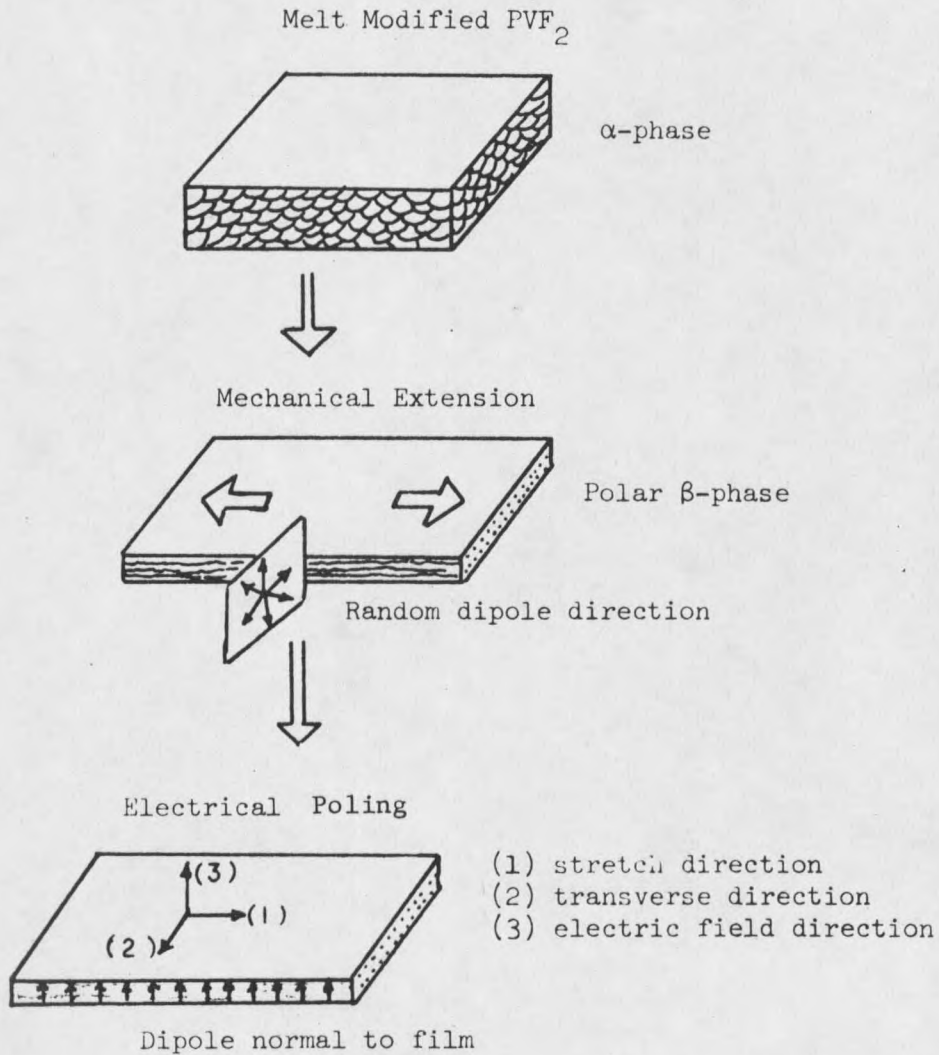


Figure 6. Schematic representation of making piezoelectric film.

We have built two kinds of rotary wind generators which use PVF₂ polymer to produce power. They employ a lateral leaf rotor and a Savonius rotor. The blades that are used in these rotors are called bimorphs. This is

because two layers of PVF₂ are glued together back-to-back to piezoelectrically induce voltages in the two sheets which add while the bimorph is bent so that one sheet is in tension and the other is in compression.

Savonius Rotor

The Savonius rotor has two blades with flexible blade roots made of a PVF₂ bimorph as shown in the Procedure section in figure 20. The change in direction of the wind force on each blade as the rotor turns will give the desired oscillation of the blades. The Savonius rotor is a non-synchronized ac generator.

It is desired to have a constant bend radius of the bimorph so that all portions of it are equally effective in generating power. Calculations show that a blade with exponentially decreasing width would attain a constant bend radius if uniform wind pressure exists over the whole blade. Now, this shape would have infinite length, so it must be truncated.

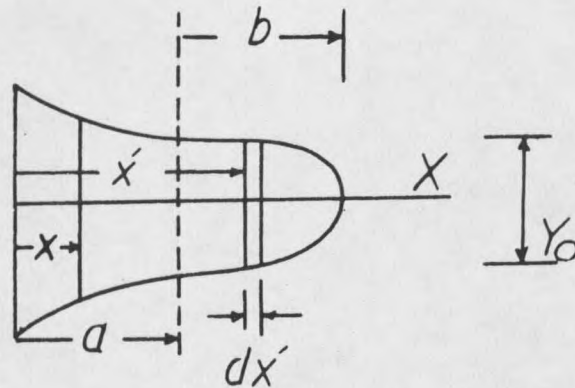


Figure 7. Blade tip shape

The following calculation supports the idea behind a particular shape. Using a parabolic shape for a truncating "cap", it is desired to get a constant torque per unit width as x varies (figure 7) which is:

$$\frac{N(X)}{Y(X)} = \frac{P}{y} \int_x^a (x'-x)y' dx' + \frac{P}{y} \int_b^a (x'-x) \frac{y_0 \sqrt{b-x}}{\sqrt{b-a}} dx' = K$$

Eq. 1

N is the torque, y is the width and p is constant. We also want with this shape a constant slope at $x=a$. Then integrating the second term on the right results in:

$$\frac{N(X)}{Y(X)} = \frac{P}{y} \int_x^a (x'-x)y' dx' + \frac{2py_0(b-a)}{3y} \left(\frac{2b+3a}{5} - x \right)$$

Eq. 2

The cap portion acts as a point source $F=2Py_0(b-a)/3$ acting at $x_0 = (2b+3a)/5$. So for any cap shape, the cap can be replaced by a force PA acting at the center of gravity of the cap.

The theoretical value of the voltage that is developed by the bimorph at a constant frequency is obtained using the fundamental piezoelectric equations and the electric displacement equation. The derivation and reasoning behind these equations are stated in the Computational Procedure section.

The current that is produced in the bimorph is equal to the time rate of change of the charge. The charge is equal to the free surface charge times the surface area A:

$$I = \frac{V}{R} = \frac{2Et}{R} = \frac{dQ}{dt} = A \frac{d\sigma_f}{dt} \quad \text{Eq. 3}$$

The electric displacement equation for a stretch in direction (1) is:

$$D_3 = \epsilon_0 E_3 + P_3 \quad \text{Eq. 4}$$

and the piezoelectric stress and strain equations are:

$$P_3 = d_{31} S_1 + (\epsilon_r - 1) \epsilon_0 E_3 \quad \text{Eq. 5}$$

and

$$\delta_1 = d_{31} E_3 + S_1 / Y \quad \text{Eq. 6}$$

For a free surface charge density:

$$D_3 = \sigma_f \quad \text{Eq. 7}$$

Substituting equation 5 into 3 gives the result:

$$\frac{dQ}{dt} = Ad \frac{ds}{dt} + A\epsilon \frac{dE}{dt} \quad \text{Eq. 8}$$

where δ is the strain, E is the electric field, S is the stress, D is the electric displacement, P is the

polarization, and Y is Young's modulus.

Substituting $\frac{2Et}{R}$ for $\frac{dQ}{dt}$ in equation 8 gives the equation:

$$\frac{2Et}{R} = Ad \frac{ds}{dt} + A\epsilon \frac{dE}{dt} \quad \text{Eq. 9}$$

A solution of the form $e^{j\omega t}$ is tried for both E and S and the following recursion relation is obtained:

$$E\left(\frac{2t}{R} - j\omega A\epsilon\right) = jAd\omega S \quad \text{Eq. 10}$$

Substitution for S from equation 5 into the above equation yields:

$$E\left(\frac{2t}{R} - j\omega A\epsilon + j\omega d^2 YA\right) = jAd\omega Y\delta$$

Using $E = \frac{V}{2t}$, we eventually obtain the recursion relation of

the following form:

$$\frac{V}{\delta} = \frac{2tAYd}{AYd^2 - A\epsilon_r \epsilon_0 + 2jt/\omega R} \quad \text{Eq. 11}$$

This calculation for δ shows the fact that while the sheet is bent, the shape achieved is a portion of a circle with radius r . The diagram is shown in figure 8.

By taking the differential of the equation for a sector, we get $dL = \theta dr$. If the displacement is also a sector with radius L then the equation is $y = L\theta/2$.

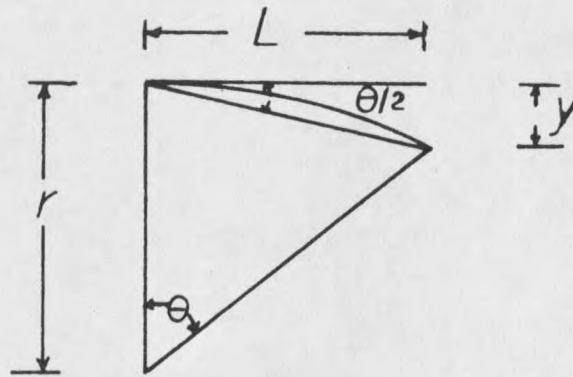


Figure 8. Geometry of deflection angle.

Now using the above equations and the relationship $dr = t/2$, we get $dL = yt/L$. Since the strain is $\delta = dL/L$, the strain in terms of L and t is $= yt/L^2$.

To find the theoretical value for voltage, we use equation 11 to get V/δ , and knowing δ , we get V .

Lateral Leaf Rotor

The reason for this design is the desirability of achieving as large a rotor as possible and also the requirement of a 60 Hz blade oscillation frequency so the power could be directly fed into the power line. The basic idea of this design which is shown in figure 35 in Appendix II is to have two blades that both have small pitch similar to that for a high-speed horizontal machine, but mounted on a vertical rotation axis. The pitch (bending) of the blade must be opposite each half revolution, and the wind force itself achieves this pitch

change as it acts on the entire blade at all times. As the wind velocity increases, the pitch will increase accordingly, tending to keep the rotor speed the same as the wind velocity increases. The bending torque tries to bring the blade back to its free position. This bending torque is quite large compared to the torque required to produce electrical power in the blade, so it becomes advantageous to get large blade deflection by having the wind pressure excite the blade at its natural frequency. This requires that the rotational frequency be equal to the blade natural (resonant) frequency.

In order to analyze the blade in the lateral leaf rotor, one has to do piezoelectric cantilever beam analysis. The exact calculation is quite complicated but an approximate approach is sufficient for a trial design. This design is later improved using a more detailed calculation made in the computational procedure section.

The cantilever blade has a thickness of $2Z_0$ and width w that is divided into two parts. The root length X_1 bends with a uniform radius R_1 and the cap of width W , thickness $2Z_0$, and length $X_0 - X_1$ is assumed to maintain a straight shape. The total blade length is then X_0 , as shown in figure 9.

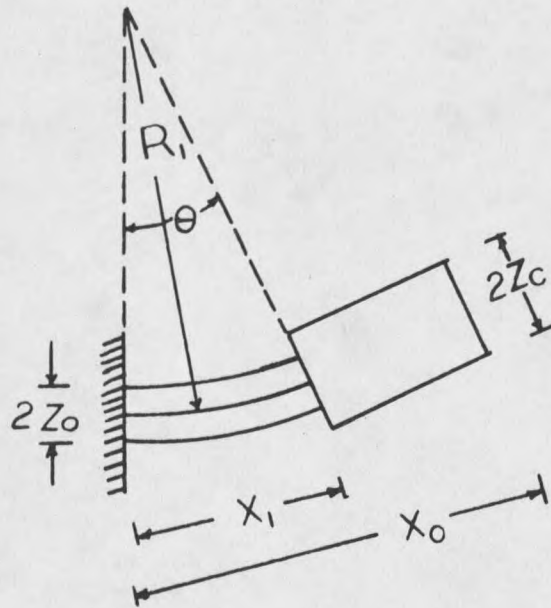


Figure 9. Cantilever blade

To compute the bending of the blade root, a uniform torque N along the root is considered and the inertia of the root is neglected, so this torque is balanced by the torque of the cantilever blade elements dz as shown in figure 10.

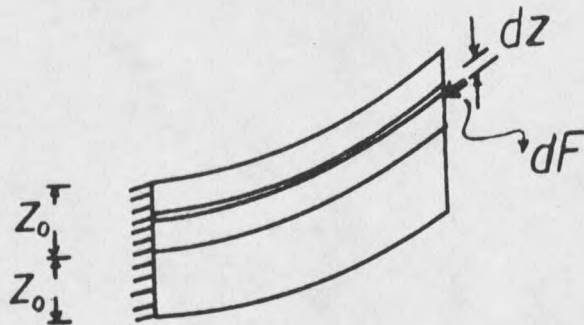


Figure 10. Cantilever torque analysis

Now, the torque is given by the equation:

$$N = \int Z dF = \int_{-Z_0}^{Z_0} ZWS(Z) dZ = \int_{-Z_0}^{Z_0} ZWY\delta(Z) dZ \quad \text{Eq. 12}$$

where S is the stress, Y is Young's modulus and δ is the strain. Now the strain $\delta = Z/R_1$ and the deflection angle $\theta = X_1/R_1$. Using the formula for root deflection, $Y_1 = \theta X_1/2 = X_1^2/2R_1$, we get $R_1 = X_1^2/2Y_1$ and $\delta = 2Y_1Z/X_1^2$. Therefore the torque,

$$N = \int_{-Z_0}^{Z_0} Z_0^2 WYy_1 x_1^{-2} Z^2 dZ = 4WYy_{11} Z_0^3 / 3x_1^3 \quad \text{Eq. 13}$$

If the blades are not connected at the tips, the centrifugal force on each blade can be considered constant and would affect the blade's radial position but not its resonant frequency, just as gravity affects the equilibrium position but not the natural frequency of a mass hanging on a spring. The blade resonant frequency is then determined from a torsional analog of Newton's second law:

$$N = 4WYy_1 Z_0^3 / 3x_1^2 = I\alpha = mx_0^2 \omega_n^2 \theta / 3$$

and

$$N = 4\rho_c Z_c \omega_n^2 y_1 W X_0^3 / 3x_1 \quad \text{Eq. 14}$$

then

$$\omega_n^2 = YZ_0^3 / \rho_c Z_c X_0^3 x_1 \quad \text{Eq. 15}$$

Now it is desired to get $\omega_r = \omega_n$, where ω_r is the angular frequency of the rotor, so there exists a synchronization between the blade's oscillation frequency

and the rotational frequency.

More generally,

$$\omega_r^2 + \omega_n^2 = \omega_o^2$$

where ω_o is the blade oscillation at zero rotor speed. If f_o is 60 Hz at resonance where $\omega_n = \omega_r$, it is important to have $\rho_c Z_c$ in accord with equation 15.

There is a new factor here that needs to be defined for a resonant blade, and that is called the quality factor or Q. If one obtains a plot of frequency of this rotor (while electrically vibrated by means of a shaker) vs. amplitude of oscillation then one obtains the following plot.

Figure 11 shows the response of the peak-to-peak amplitude of a sample vs. the applied frequency. It also shows the bandwidth at half power corresponding to amplitude of oscillation $1/(2)^{\frac{1}{2}}$ of its maximum value, that is:

$$\frac{\text{R.F.}}{f_2 - f_1} = Q$$

where R.F. is the resonant frequency and f_2 and f_1 are obvious from the plot.

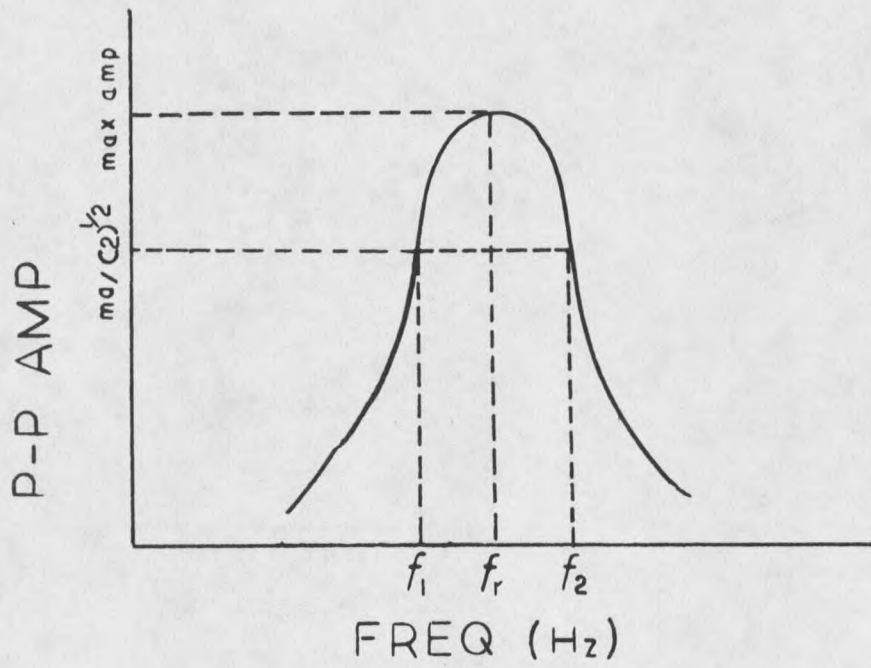


Figure 11. Frequency vs. amplitude response

For a driving force $F_0 \cos \omega t$, the displacement is Q times as large as the displacement for a static force F_0 . Therefore, a resonantly driven blade can be much thicker and produce more piezoelectric power than a nonresonant blade.

Energy Analysis

The quality factor Q is also a measure of the energy stored in a resonant system divided by the energy lost per radian. The fraction of energy lost per cycle is $2\pi/Q$. This energy must be supplied by the windstream to retain a constant amplitude of oscillation. The mechanical energy in the PVF2 blade root is computed as follows:

1st: Energy density = $S\delta/2 = Y\delta^2/2$ and $\delta = \delta_0 Z/Z_0$

2nd: For two blades this mechanical energy is the integral of the energy density:

$$E_{\text{stored}} = \int_{-z_0}^{z_0} WX_1 Y (\delta Z/Z_0)^2 dZ$$

Now the power loss is $E_{\text{stored}} \omega/Q$. The power due to the kinetic energy of the windstream incident on the rotor's projected area is

$$P_{\text{in}} = \rho_a WRU_0^3$$

From the relations given in the Computational Procedure section, we get for the output power:

$P_{out} = V_o^2 \omega C / 4$ where $v_o = gY\delta_o Z_o$, and $C = \epsilon W X_1 / 2Z_o$ for one blade. Here V is the peak open circuit voltage and C is the blade capacitance. This formula assumes an impedance-matched resistive load. The efficiency, P_{out}/P_{in} , and internal losses are computed and shown in the Procedure section.

CHAPTER 3
PROCEDURE AND TESTS

In order to obtain the best PVF_2 polymer for our rotors we measured mechanical properties of samples from various manufacturers so as to choose a polymer of higher quality. In doing so, we achieved better electrical power output as well as mechanical responses.

The first series of tests were performed to obtain Young's modulus, yield strain and piezoelectric strain coefficients. The experimental set-up is shown in figure 2⁸ of Appendix I. In order to make the measurements of the above constants, the following circuit was designed.

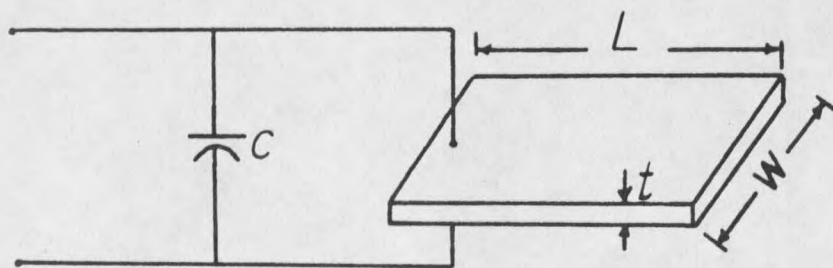


Figure 12. Circuit to measure Y , d_{ij} .

To obtain Young's Modulus, we start with the basic equation of:

$$Y = \frac{\text{stress}}{\text{strain}} = \frac{S}{\delta}$$

where $S = \frac{F}{A} = \frac{F}{wt} = \frac{mg}{wt}$

and strain is $\delta = \frac{\Delta l}{l}$. Now, m is the load mass creating tension in the wire, g is acceleration of gravity, l is the length of the sample, Δl is the change of length, w is width of the sample and t is the thickness.

The fundamental piezoelectric and electric displacement equations are used to calculate the piezoelectric strain constant. They are the following:

$$P = S \cdot d + \epsilon_0 (\epsilon_r - 1) \cdot E, \quad \text{Eq. 1}$$

$$\text{and } D = \epsilon_0 E + P, \quad \text{Eq. 2}$$

where P is the polarization vector due to the applied stress S (stress tensor), E is the electric field vector, D is the electric displacement vector, ϵ_r is the dielectric tensor, and d is the piezoelectric strain tensor.

Now substitution of P from equation 1 into equation 2 results in the relation

$$S \cdot d = D - \epsilon \cdot E, \text{ where } \epsilon = \epsilon_0 \epsilon_r \quad \text{Eq. 3}$$

In our application the direction of the applied stress is 1 and the desired field is produced in the 3

direction. This simplifies equation 3, because only one piezoelectric strain coefficient d_{31} is needed:

$$d_{31}S_1 = D_3 - \epsilon_{33}E_3 \quad \text{Eq. 4}$$

The stress is the force per area, so $S_1 = \frac{mg}{wt}$. Also the electric field in the dielectric is the voltage divided

by the thickness, $E_3 = \frac{V}{t}$.

The electric displacement in the dielectric is equal to the free surface charge density, $D_3 = \sigma$. The free surface charge density is also equal to the total charge divided by the surface area, $\sigma = \frac{Q}{w_1}$ or $D_3 = \frac{Q}{w_1}$. The total charge is also equal to the voltage divided by the capacitance C .

Now substitution of the above values in equation 4 results in

$$d_{31} = \frac{VtC}{mgl} - \epsilon_0 \epsilon_r \frac{Vw}{mg} \text{ or } \frac{V}{mg} = \frac{d_{31}}{\frac{tC}{l} - \epsilon_0 \epsilon_r w}$$

A plot of mg vs. V (voltage) developed across the PVF₂ is shown in the Appendix 1, figure 30. The slope of that line is proportional to d_{31} .

The complete apparatus figure for this experiment is presented in figure 28 of Appendix 1.

Test Procedure for Determining Natural Frequency and Quality Factor Q

Since the energy loss in our system greatly depends on Q, a careful measurement of this quantity is necessary. The energy loss is determined by Q, so the higher Q is, the less lossy the system. The basic physics of Q is mentioned in the Theory section.

Natural frequency and quality factor Q for PVF₂ bimorph was determined by electrical excitation. The circuit that was used is shown in figure 32 of Appendix I. The variable frequency oscillator was operated at various frequencies and constant amplitude. Then the corresponding amplitude as result of change in frequencies was measured. The oscillator output was amplified through the power amplifier and then fed into the shaker. The rotor natural frequency was measured by mounting the ends of the central rod on the shaker so the blades were perpendicular to the direction of vibration and then the amplitude of oscillation was measured by means of a stroboscope. The method of finding Q and resonant frequency is explained in the Theory section. The measurements of natural frequency of the oscillator leaf were a little different. First the blade itself was mounted on a strip of rigid aluminum and then vibration applied so the natural frequency of the blade was

measured. Then the blade was mounted on the spring steel and the length was adjusted so that the entire outfit could oscillate with the natural frequency of the blade measured previously. This length was used in the wind tunnel. Sometime the second mode of vibration was measured if it was appreciable. This second mode also occurs at the same length of the spring steel.

Blade thickness calculation for lateral leaf rotor:

This computation assumes the rotor is turning with some frequency f by the wind force. The wind speed is u at all times. The following diagram shows variables and constants for this computation

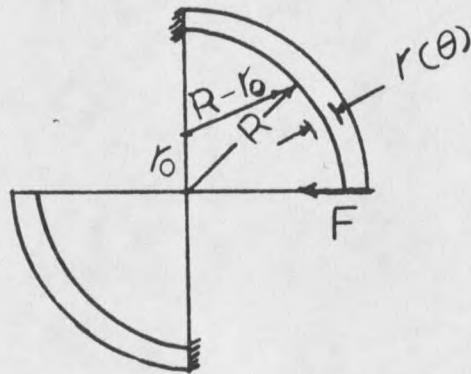


Figure 13. Geometry of blade root.

The calculation for maximum kinetic energy follows:

$$r(\theta, t) = r(\theta) \cos \omega t$$

where $r(\theta) = r_0(1 - \cos \theta)$

$$v(\theta, t) = -\omega r(\theta) \sin \omega t$$

$$\text{so } KE_{\max} = 1/2 \int m v_{(\theta)}^2 d\theta$$

Eq. 5

$$KE_{\max} = \rho Z_0 r_0^2 \omega_0 R \omega^2$$

Let $KE_{\max} = PE_{\max}$ to get the thickness h .

Then after a lot of derivation and substitution

$$h = \sqrt{\frac{(5/3 - \pi/2) \rho}{y} \frac{u^2 r_t^2}{\omega_0^2}} \quad \text{Eq. 6}$$

where ρ is density of PVF₂, u wind velocity, r_t tip speed ratio, and ω_0 is the line frequency of 377 rad/s.

$$R \omega_0 = u r_t$$

then $R = \frac{u r_t}{\omega_0}$ cm. Our particular design requires $R = 2.65$

Now the second part of the calculation is to find the parameter α in the following blade shape equation:

$$W = M \sin \alpha \phi \quad \text{Eq. 7}$$

where M is blade height, α is a constant, and ϕ is blade shape angle. To do so, we use the geometric equation, force balance and torque balance equation for the blade.

$$\text{They are: } dT = -\hat{\rho} T d\phi + \hat{\phi} \frac{\partial T}{\partial \phi} d\phi \quad \text{Eq. 8}$$

$$dc = \hat{\phi} c d\phi + \hat{\rho} \frac{\partial c}{\partial \phi} d\phi \quad \text{Eq. 9}$$

$$dT + dc + dF_c = 0 \quad \text{Eq. 10}$$

$$\left(-T + \frac{\partial c}{\partial \phi} + BW\right) \hat{\rho} + \left(\frac{\partial T}{\partial \phi} + c\right) \hat{\phi} = 0 \quad \text{Eq. 11}$$

$$dN = \hat{k} R c d\phi \quad \text{Eq. 12}$$

where T is tension, c is shear force, N is torque, F_c is centrifugal force, and B is a constant. With proper boundary conditions and substitutions of one equation

into another, the simplified forms of the equations used are stated as:

$$\frac{\partial T}{\partial \phi} + \frac{1}{R} \frac{\partial N}{\partial \phi} = 0 \Rightarrow T = -\frac{N}{R}$$

$$N = DW \text{ for constant curvature, so } T = -\frac{D}{R} W$$

where D is constant. These result in the following differential equation

$$\left(\frac{D}{R} + B\right) W + \frac{D}{R} \frac{\partial^2 W}{\partial \phi^2} = 0 \quad \text{Eq. 13}$$

A solution of the above is

$$W = M \sin \alpha \phi + n \cos \alpha \phi .$$

From boundary condition $n=0$,

$$W = M \sin \alpha \phi \quad \text{Eq. 14}$$

In finding α , there are tremendous calculus and engineering mechanics involved, so here we just state the results of those calculations:

By the means of the previous equation, α is shown to be

$$\alpha = \sqrt{1 + \frac{BR}{D}} \quad \text{or} \quad \alpha = \sqrt{1 + \frac{3R^4 \omega^2 \rho_0}{YZ_0^2}} \quad \text{Eq. 15}$$

The plot of α vs ω is shown in figure 34 in Appendix II.

Calculation of elastic energy of the PVF₂ blade shows

$$U_e = \frac{YMZ_0^3}{Ra} (1 - \cos \alpha \phi_0) \quad \text{Eq. 16}$$

Centrifugal energy is

$$U_c = \rho^2 \omega^2 M (2Z_0) R r_0^2 \left[\frac{3}{2a} (1 - \cos \alpha \phi_0) - \frac{a(\cos \alpha \phi_0 - \cos 2\phi_0)}{a^2 - 4} + 2a \frac{(\cos \alpha \phi_0 - \cos \phi_0)}{a^2 - 1} \right]$$

It can easily be shown that a depends on ϕ in the following manner,

$$3a^4 - 21a^2 + 36 + (-a^4 + 7a^2 - 18) \cos \alpha \phi_0 + 2a^2(a^2 - 1) \cos^2 \phi_0 - 4a^2(a^2 - 4) \cos \phi_0 = 0 \quad \text{Eq. 17}$$

for $\phi_0 = 90^\circ \Rightarrow a = 1.6$. Now all the parameters in the design consideration are found, so a particular shape is obtained through some tedious calculation.

Electrical Analysis of Lateral Leaf Rotor

The lateral leaf rotor is based on the following computations and analysis, and is shown in figure 35 in Appendix II. In making this analysis, we considered a bimorph with outer layers of piezoelectric polymer and center layer of plastic with negligible density and stiffness, just strong enough to make the blade act as a beam.

It is considered that this bimorph is feeding a line whose voltage is lower than that of the bimorph. So the circuit is as follows:

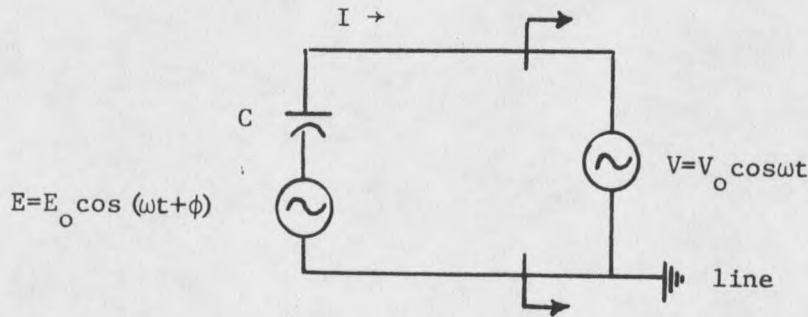


Figure 14. Capacitive blade generator.

By adding the voltages around the loop according to Kirchhoff voltage law, I is found,

$$I = \frac{\sum E_i}{Z}$$

$$I_0 = j\omega C(E_0 \angle \phi - V_0), \text{ so}$$

$$I = \omega C(-E_0(\sin \omega t \cos \phi + \cos \omega t \sin \phi) + V_0 \sin \omega t)$$

$$\text{Average power} = \langle P \rangle = VI^*/2 = -\omega C V_0 E_0 \sin(\phi)/2$$

Maximum power is when $\phi = -90^\circ$, but I is then not in phase with V . To have I in phase with V as desired by the utility company,

$$-E_0 \cos \phi + V_0 = 0 \text{ or } \cos \phi = \frac{V_0}{E_0}$$

$$\langle P \rangle = - (1/2) \omega C V_0 E_0 \sin[\cos^{-1} \frac{V_0}{E_0}]$$

$$\text{Then } \langle P \rangle = (1/2) \omega C V_0 \sqrt{E_0^2 - V_0^2} \quad \text{Eq. 18}$$

Now if the blade is considered as a current generator, consisting of very thin layers of thickness dz stacked together, we have the following equivalent circuit:

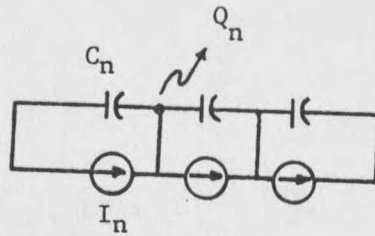


Figure 15. Blade as current generator

$$\text{Therefore } I_n = A \frac{d}{dt} [dx_n + (\epsilon - 1)E_n]$$

$C_n = \epsilon A / dz$. It is known that I_n varies with n , so Q_n will be an additional variable.

After using the fact that $V = ZI$

$$V = [dx + (\epsilon - 1)E] Z_o / \epsilon$$

The blade considered as a voltage generator has the following equivalent circuit:

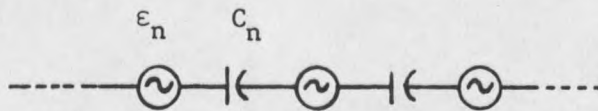


Figure 16. Blade as voltage generator

A Thevenin and Norton analysis of the blade results in

$$Z_{eq} = \frac{V_{th}}{I_{Nor}} = j \frac{Z_o}{\omega \epsilon A}$$

In terms of strain the impedance increased by a factor of

$$\frac{1}{1 - \frac{d^2}{\delta \varepsilon}} \text{ so, } Z = - \frac{jZ_0}{\omega \varepsilon A} \frac{1}{1 - \frac{d^2}{\delta \varepsilon}}$$

Using the stress equation, the impedance is again of the form

$$- \frac{jZ_0}{\omega \varepsilon A}$$

Again calculation of mechanical energy by using strain and stress equation for a blade of thickness $2Z_0$ would result in:

$$\langle W_m \rangle = \frac{w l \omega \varepsilon V_0 \sqrt{E_0^2 - V_0^2}}{2Z_0}$$

Now if the blade circuit is inductive as well as capacitive, it is represented by the following figure.

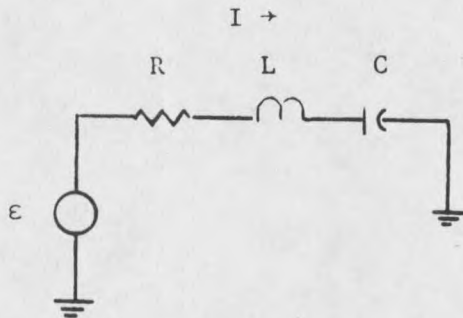


Figure 17. RLC representation of generator

so if ω is close to ω_0 , defined as $(LC)^{-1/2}$,

$$I = \frac{\epsilon}{j2 \frac{\omega - \omega_0}{\omega_0} QR + R}$$

where

$$Q = \frac{\omega_0 L}{R}$$

The inductor energy is $\frac{1}{2}LI^2$ and the energy loss per radian is $I^2R/2\omega$.

Now the efficiency of blade for the parallel case is of the form $\text{eff} = 1/Q_{\text{elc}}(1/Q_{\text{elc}} + 1/Q_{\text{mech}})$

$$\text{where } 1/Q_{\text{elc}} = \frac{\Delta E_{\text{elc}}/\text{radian}}{E_m}$$

The data that shows the power and voltage output of this design is included in Appendix II.

To measure power output of the lateral leaf rotor generator, the following circuit is used:

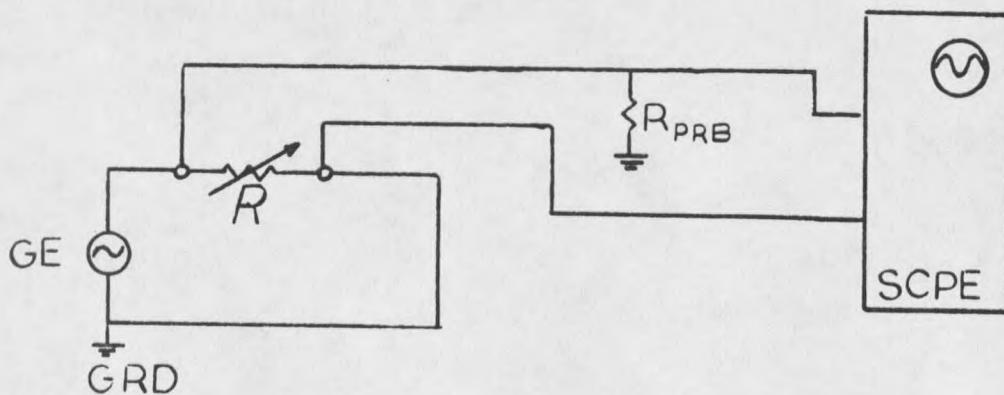


Figure 18. Impedance matching circuit for the generator power output.

R is a variable resistor box model 1100 made by EICO. The oscilloscope is Model T922 made by Tektronix. R_{probe} is 10M ohm.

The power output vs. the resistance of the box plotted for the wind velocities of 9.6, 11.6, 14.3 and 22 m/s is shown in figure 19. The maximum power output of this generator is 750 μw at a wind velocity of 22 m/s.

$$\text{Now the power is } \frac{V_{\text{p-p}}^2}{8R}$$

where $V_{\text{p-p}}$ is peak-to-peak voltage of the generator

$$\text{and } R = \frac{(R_1)(R_{\text{probe}})}{R_{\text{probe}} + R_1}$$

For the case of $R_{\text{probe}} \gg R_1$, R is just the resistance of the box.

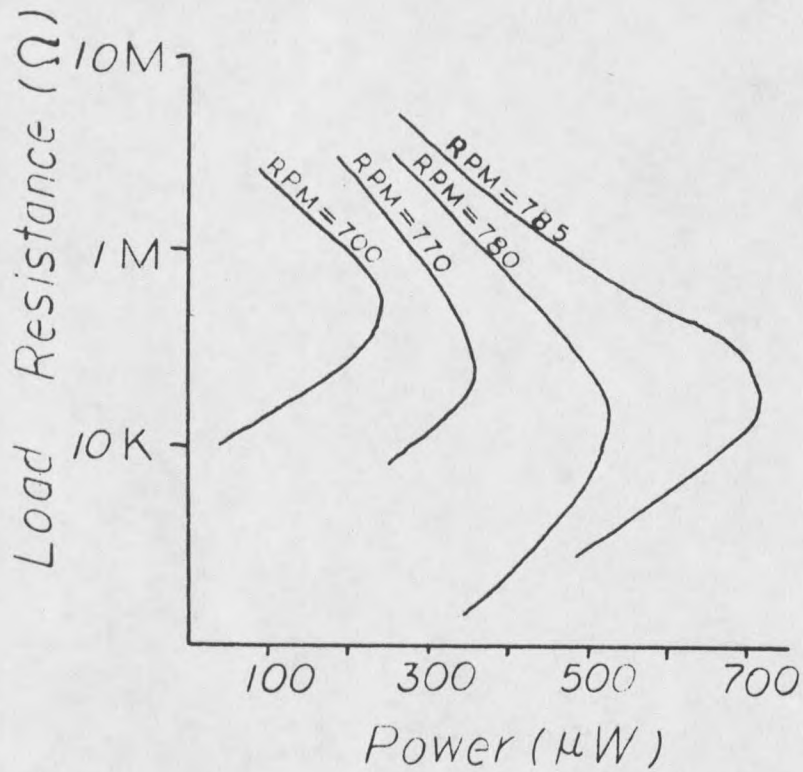


Figure 19. Power vs. load resistance curves

In summary from both the Theory and Procedure sections the lateral leaf rotor power design requirements are

- A. Develop an oscillating blade
- B. Find the mechanical energy needed to bend blade
- C. Determine the fraction of energy going to stored mechanical energy
- D. Determine the fraction of energy going to electrical energy
- E. Calculate internal energy lost and friction

- F. Determine how the above statements are related to electromechanical coupling constant.
- G. Determine the role of dielectric constant
- H. Decide on series or parallel blade connections

Savonius Rotor

The basic physics of this design is explained in the Theory section. This rotor is basically a drag-type rotor. In addition to drag on the vane producing rotary shaft power, that drag creates down wind forces on the tower.

The S-rotor which is subject to the Magnus effect slows air down on one side while speeding it up on the other. The diagram below shows the basic shape of our Savonius rotor which has a fairly high tip speed ratio, almost 1.

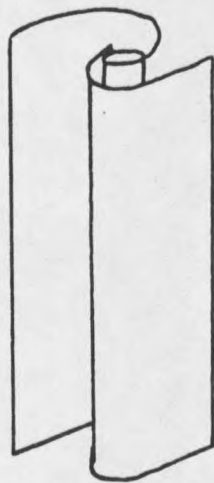


Figure 20. Savonius rotor design for oscillating blades.

In order to get a high RPM from a S-rotor, two considerations ought to be taken into account:

1. Maximize the difference in drag coefficients between upwind and downwind vanes, and
2. Minimize the wind force against the upwind moving vane. These two requirements can be met by a proper design of shapes like cone, wedges, extra vane, etc.

The S-rotor oscillating blade for application of PVF₂ is a little different than the regular S-rotor for rotary shaft power.

This S-rotor was built by the wind generator lab in the following manner. The generator frame consists of two thin-walled tubes. Each tube has a diameter of approximately one half the length of the active region of one side of the bimorph. The tubes are connected together by two nylon bolts. These tubes have a brass rod with a cone-shaped tip connected at each end.

The brass rods are electrically insulated from each other and serve as bearings which also carry current to the external circuit. The bimorph that was constructed for the S-rotor is two layers of PVF₂ glued together back-to-back so the piezoelectrically induced voltages in the two sheets add when the bimorph is bent so that one sheet is in tension and the other is in compression. The

two sheets were connected with epoxy glue. The hardener was placed on one surface and the resin was placed on the other surface. The hardener and resin were cleaned completely off and the sheets were then placed together. A top view of the S-rotor with the bimorph mounted on its center rod is shown in figure 21.

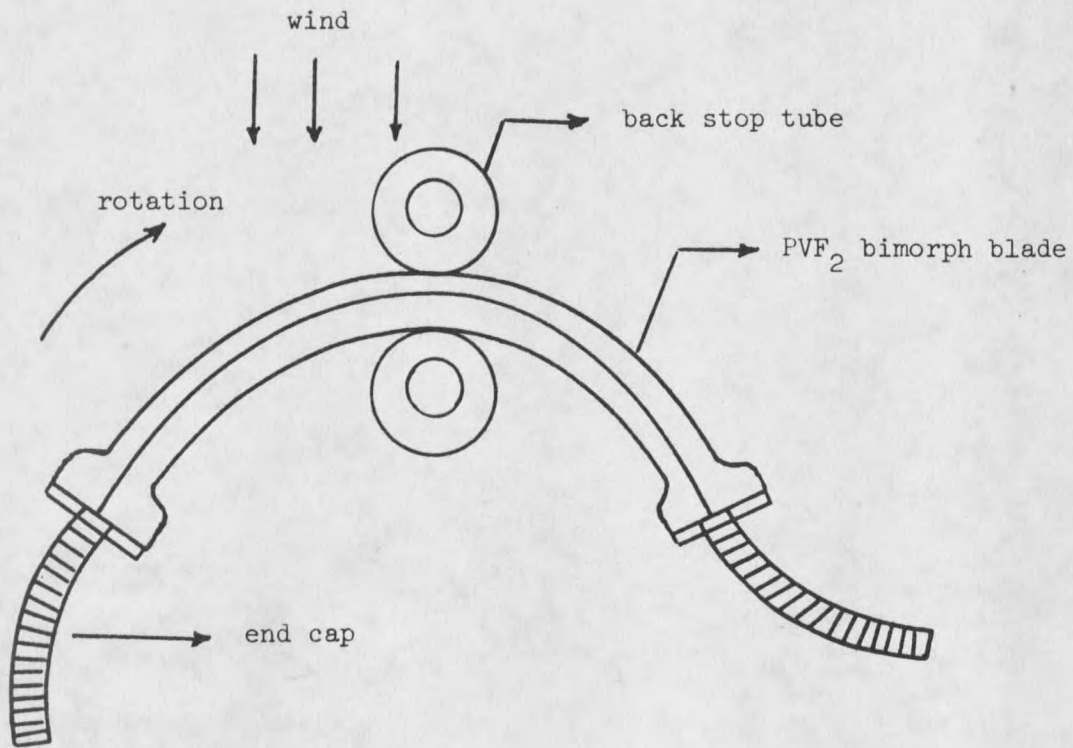


Figure 21. Top view cross section of Savonius rotor with PVF₂ bimorph.

The electrical measurements were recorded by an oscilloscope with a variable resistor box connected in

parallel to the leads. The output power vs. the load resistance is shown in figure 22.

The maximum output is $95.2\mu\text{w}$ at a load resistance of $4.12\text{M}\Omega$. The deviation of experimental results from the theoretical results is due to the use of the actual bimorph area in the calculations. A smaller effective area should be used as the bimorph was not uniformly strained as assumed.

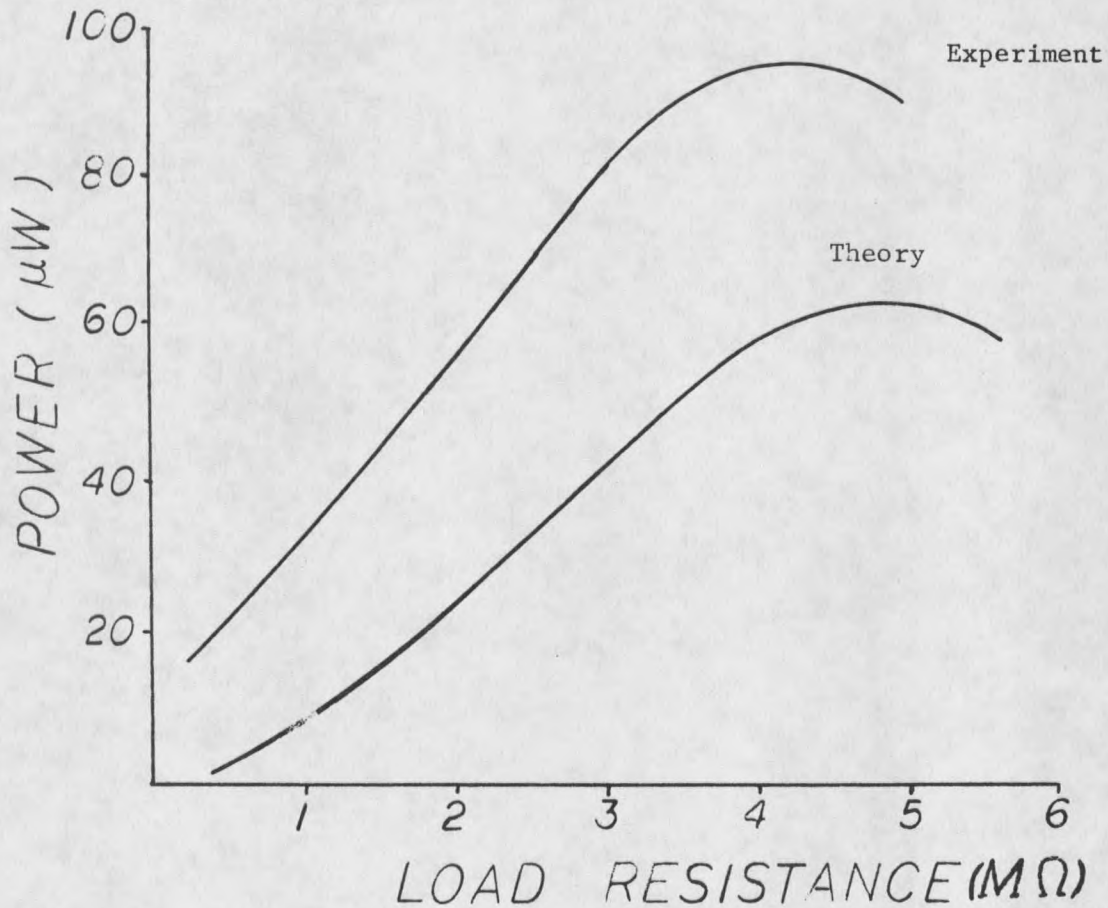


Figure 22. Plot of power vs. load resistance of S-rotor generator.

The design parameters of the Savonius rotor are found for arbitrary PVF₂ thickness t and blade width w . Numerical results here are for $t=100$ microns and $w=10$ cm, and a wind speed for this design is $V_0=10$ m/sec. This wind velocity is the required value to bend the blade to its minimum radius as limited by the back stop tube. The steps in the Savonius rotor analysis are:

1. Calculation of allowable strain δ_{max}
2. Calculation of allowable curvature R_{min}
3. Calculation of allowable torque T_0 needed to obtain R_{min}
4. Calculation of blade length L required to achieve T_0 at design wind speed V_0
5. Computation of blade oscillation frequency f_0 at design wind speed V_0
6. Computation of blade open circuit voltage V_0 when bent to radius R_{min}
7. Calculation of blade electrical impedance Z .
8. Measurements of power per cm^3 of PVF₂ volume at design wind speed V_0
9. and calculation of output power per m^2 of intercepted wind area of V_0 .

Oscillating Flag Generator

This is the newest idea in application of PVF₂ in a

wind generator. The rotor is eliminated, and replaced by a cantilever-mounted blade which oscillates at its natural frequency. The first idea was to develop a design like a tree leaf which oscillates back and forth in the wind. The second idea comes from a road sign, which shows oscillation of the entire sign and its mount together. The combination of these two ideas led to the design of the oscillator leaf generator. The basic construction involves a flexible piece of plastic cut in the shape of a tree leaf mounted on a thin spring steel strip that is set into oscillation by the wind force. Our first design with PVF₂ glued back-to-back onto the neutral layer didn't oscillate by itself due to the change in the mechanical properties of the composite. The gluing stiffened the entire blade, creating a less flexible leaf which could not oscillate. This problem was overcome in two stages:

A. First, by covering only one-fourth of the blade with PVF₂ glued back-to-back with double sided scotch tape.

B. Second, by designing a vortex maker in the shape of a cylinder that had its diameter half of the blade length, so it could deflect wind off its side to easily pull the blade tip in and then out. This helped the blade and the spring steel to oscillate with much bigger

amplitude and greater bending at the blade root.

A sample model of this generator leaf and its construction are shown in figures 23 and 24.

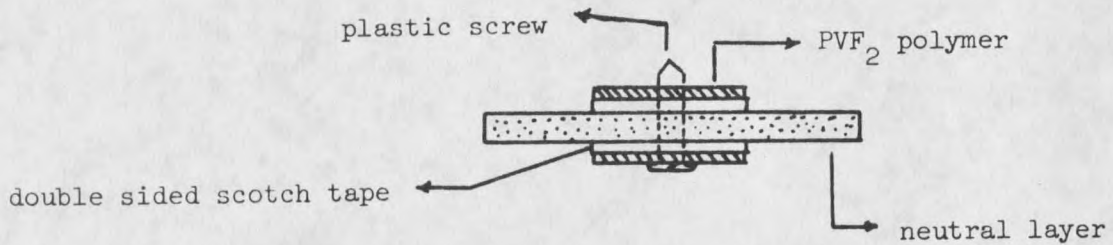


Figure 23. Cross section of oscillator leaf

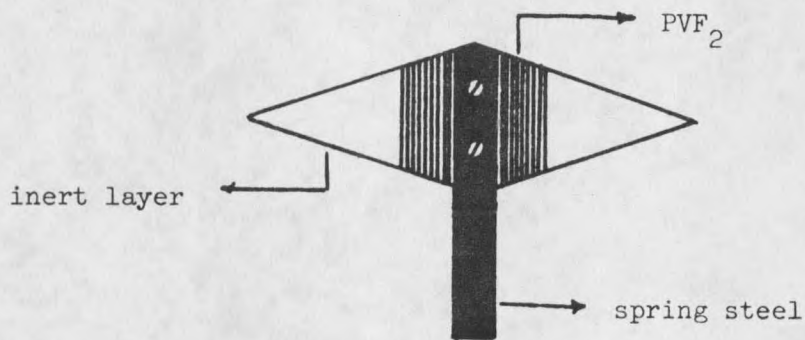


Figure 24. Front view of an oscillator leaf

Again the power output was measured by an oscilloscope with variable resistor connected in parallel to the leads. The maximum power was obtained for resistance of 3.2 M ohms. The maximum power was 10 μ W for a very small area of PVF₂. The area of PVF₂ used was 6 cm² on each side of the neutral layer. In figure 25 the plot of R vs. power output is shown for three

different velocities. The resonant frequency of this blade was 25.5 Hz. The change in the resonant frequency as result of change in wind velocity is about ± 1 Hz.

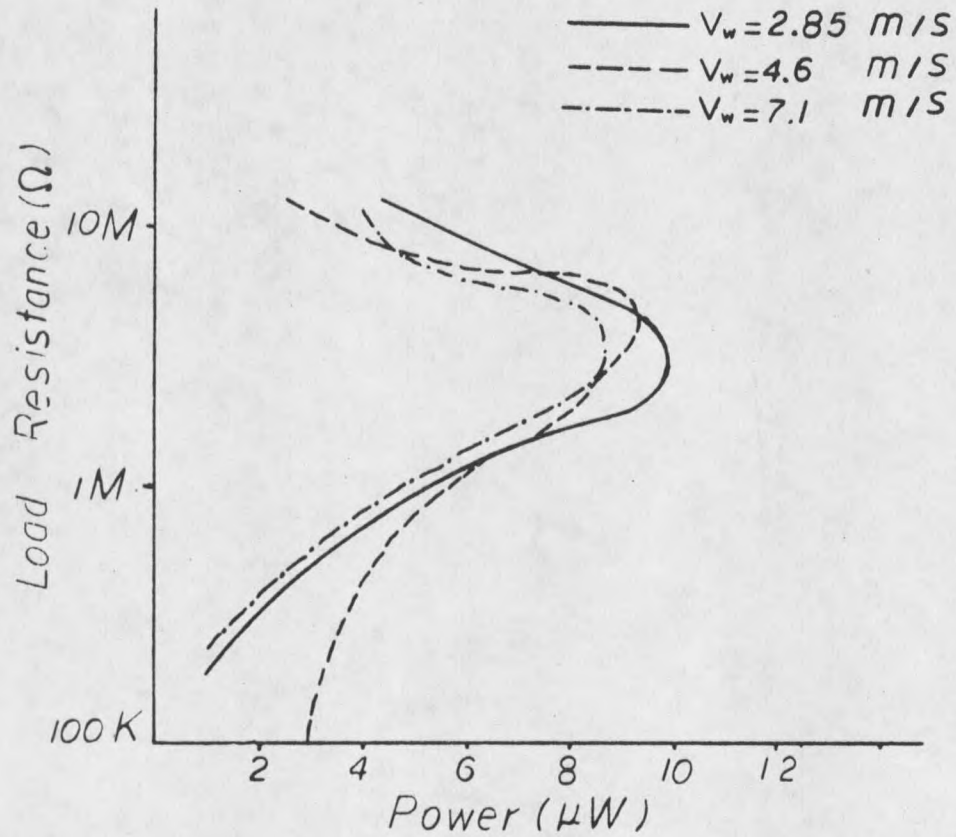


Figure 25. Output power vs. load resistance for oscillating leaf

The generator as recently made consisted of a thin steel leaf spring mounted as a cantilever (thickness 0.02 in) with a blade attached near its tip. The blade was made of plastic which was 230 micron thick. Two layers of PVF₂ polymer with thickness of 28 micron were attached on either side, near the blade's central portion. The blades extend outward from the tip of the steel spring like two wings, in a T configuration. With no wind blowing the entire assembly lies in a vertical plane. With wind blowing perpendicular to this plane, the spring bends and both blade tips bend backward before the assembly goes into oscillation. When the oscillation starts, it does so at this bent-back equilibrium position. The back and forth oscillation is relative to that equilibrium position. The blade tips oscillate with respect to their equilibrium condition. The blade and the spring do not oscillate in phase. To find the phase relationship of this oscillation, a series of pictures were taken by means of a stroboscope. Different blade shapes have different phase relationships.

The reason for oscillation and cycle of operation are as follows:

- 1) The spring begins at its rearward (wind is blowing against its back) position but the blades are in their neutral curved

configuration. Now as the blade goes forward in the direction of the wind, the blade tip goes rearward straightening the blade so as to provide the maximum cross section toward the wind by the time the spring has gotten to its equilibrium position.

- 2) The spring keeps moving forward from its neutral to its most forward position while the blade continues forward to its equilibrium position (both motions are relative to the spring).
- 3) The spring comes back to its neutral position, while the blade moves forward relative to the spring, thus providing the wind with the smallest area, at the time when the spring motion toward the wind is greatest.
- 4) The spring continues going rearward to its rear most position finishing the cycle while the blade tips go rearward to their neutral configuration.

If small amplitude of oscillation is considered, the blade gets more energy from the wind while going forward than it gives up while coming back to its neutral position. This is because the area which the wind pushes on is larger during the forward motion. As the amplitude of oscillation gets larger, the wind velocity against the

blade becomes smaller during the forward motion and faster during the rearward part of the cycle. This tends to decrease the net energy input per cycle, but this is compensated by greater bending of the blade produced by the greater wind velocity difference resulting from the increase in area difference between the forward and rearward motion.

At last the blade bends so far at the extremes of its motion that more bending hardly increases the area differential any more. For this amplitude the energy input and loss per cycle becomes the same and the amplitude of oscillation stabilizes.

Line Synchronization Calculation

To synchronize the PVF₂ blade to 60 Hz cycle operation, the coupling of PVF₂ to the ac line should be considered in detail. An estimate is presented of a simple criterion for frequency locking. It is thought that the oscillator will choose the frequency of oscillation which gives maximum amplitude. Consider the blade is oscillating with a given amplitude x_0 at resonance. Now \bar{x}_0 , the amplitude of a forced damped harmonic oscillator driven at frequency ω is as follows:

$$\bar{x}_0 = F_0/m[(\omega_0^2 - \omega^2)^2 + \omega^4/Q^2]^{1/2} \quad \text{Eq. 19}$$

If it is assumed that oscillation takes place at the

frequency ω_0 , which is the resonant frequency of the undamped system, then Eq. 19 becomes

$$x_0(\text{res}) = F_0 / (m\omega^2 / Q') \quad \text{Eq. 20}$$

where Q' includes both the mechanical losses and the electrical output at resonant frequency ω_0 from the PVF₂ blade.

Since the resonant frequency is different from the line frequency ω , and the line has basically zero impedance, the electrical power dissipated in the source resistance R is ϵ^2 / R , where ϵ is the rms source emf (voltage generated by the bimorph).

If the blade locks into the line frequency, then equation 19 applies. This way Q differs from Q' in that the electrical output is smaller because the generator is supplying the line. For a value of ω_0 in which both expressions for x_0 in equations 19 and 20 are equal, Q is sufficiently larger than Q' so that the other term which appears only in equation 19 is compensated.

This equality takes place when $\Delta\omega/\omega = (k^2/4Q)$ where $\Delta\omega$ is the magnitude of the frequency difference between ω_0 and ω , and k^2 is the electromechanical coupling constant which is about 0.01 for PVF₂. Since Q is about 20 for the blades we have measured, this relation says that there can be about 5% deviation of the resonant frequency from the line frequency before the blade gets

out of synchronism with the line frequency. This supports the idea that the blade is to be designed for maximum power output. In our measurements the frequency stability as wind velocity changes over a wide range is about 1% so obtaining synchronization with the line seems to be a possibility.

Computational Procedure for Line Synchronization

The basic assumptions that one needs to make are as follows:

1. The blade oscillates at the frequency at which its amplitude is largest. The amplitude x_0 of oscillation remains the same regardless of whether it is at resonance with the line ($\omega_1=377$ rad/S) or resonant at the blade natural frequency ω_0 .

2. The driving force amplitude F_0 of the wind is the same at ω and ω_0 as long as the blade amplitude remains the same at $x_0(\omega_1)$ and $x_0(\omega_0)$.

3. This x_0 is given by the standard driven damped harmonic oscillator expression

$$x_0 = F_0/m[(\omega_0^2 - \omega^2)^2 + \omega^4/Q^2]^{1/2}$$

Now for $\omega=\omega_0$ the above relation is

$$x_0 = F_0 Q_0 / m \omega_0^2$$

If Q is not dependent on ω then this value $\omega=\omega_0$ will result in the maximum x_0 . Basically Q is limited by both

mechanical and electrical losses. It is also considered that Q_m is independent of ω .

As earlier in this section, we consider the blade as a voltage generator with series capacitive impedance. If a lot of blades are connected in parallel then connecting an inductor in series with these blades will reduce the impedance and make it more resistive. Figure 26 shows three generators connections in parallel.

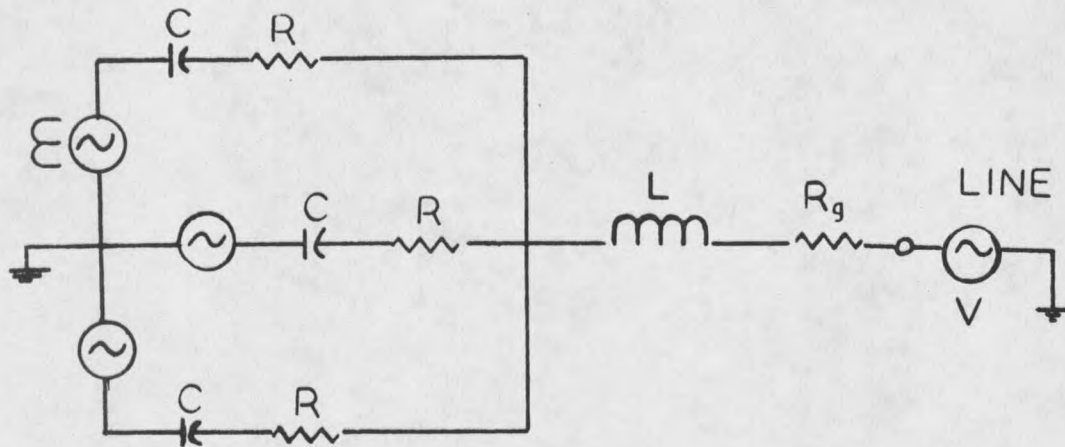


Figure 26. Circuit representation of three generators in parallel.

Now based on the above conditions, the circuit in figure 26 reduces to the circuit in figure 27.

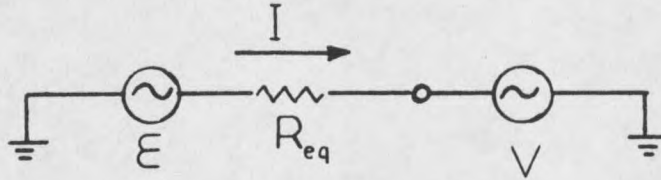


Figure 27. Equivalent circuit of figure 26.

The line has a voltage of V and zero impedance. Since the voltages are ac then we have

$$E = E_0 \sin \omega t \text{ and } V = V_0 \sin \omega_1 t$$

In the first case, it is assumed that $\omega \neq \omega_1$ therefore the power output is simply $\epsilon_{\text{rms}}^2 / R_{\text{eq}} = \epsilon_0^2 / 2R_{\text{eq}}$ which is also the power loss.

This is supported by the following derivation:

$$\text{Heat loss in } R_{\text{eq}} \text{ is } \int_0^T (\epsilon - V) I dt = \int_0^T \frac{(\epsilon - V)^2}{R_{\text{eq}}} dt$$

After substitution of $\epsilon(t)$ and $V(t)$ into the above relation and integrating it, the heat loss is given by

$$H \cdot L_u = T \left[\frac{\epsilon_0^2}{2R_{\text{eq}}} + \frac{V^2}{2R_{\text{eq}}} \right] \quad \text{Eq. 21}$$

Equation 21 exhibits the heat contribution from the line and the generator to the load separately. The second case is when $\omega = \omega_1$ so both line and generator are synchronized. Now the heat loss calculation in the load

is coupled such that

$$H \cdot L_s = \frac{T}{2} \frac{(\epsilon_o - V_o)^2}{R_{eq}}$$

The real power into the line is,

$$\langle IV \rangle = \frac{1}{2} \frac{(\epsilon_o - V_o) V_o}{R_{eq}}$$

Addition of power losses results in the power output of generator ϵ or

$$W = \frac{1}{2} \epsilon_o (\epsilon_o - V_o) / R$$

Q Calculation for Synchronized and Unsynchronized Cases

It is known that the mechanical energy stored in blade is

$$W_m = \frac{1}{2} Y S^2 A t$$

where A is area and t is thickness of blade.

The voltage ϵ of the generator as seen previously is

$$\epsilon = -Y \frac{dSt}{\epsilon}$$

From the definition of Q it is obvious that

$$Q_u = \frac{\omega Y S^2 A t R_{eq}}{\epsilon_o^2} \quad \text{Eq. 22}$$

$$Q_{elc} = \frac{1}{\omega R_{eq} C} = \frac{t}{\omega R_{eq} \epsilon A} \quad \text{Eq. 23}$$

Now by manipulating equations 22 and 23 it can be shown that:

$$Q_u = \frac{1}{k^2 Q_{elc}} \quad \text{Eq. 24}$$

Similarly

$$Q_s = \frac{\epsilon_o}{k^2 Q_{e1c} (\epsilon_o - V_o)} \quad \text{Eq. 25}$$

Using equations 19, 22, 23, and 25, substitution back and forth results in:

$$\frac{\omega_o^4}{Q^2} = \frac{\omega_1^4}{\left(\frac{1}{Q_m} + \frac{1}{Q_u}\right)^{-2}} \quad \text{Eq. 26}$$

After a lot of algebra and a binomial expansion, equation 26 can be written as

$$\frac{(\omega_o - \omega_1)^2}{\omega_1^2} = \frac{1}{4} \left[\frac{k^2 Q_{e1c}}{Q_m} + \frac{3}{4} K^4 Q_{e1c}^2 \right] \quad \text{Eq. 27}$$

Using numerical values from our first design such as $k^2 = 0.01$, $Q_{e1c} = 20$ and $Q_m = 20$, we obtain

$$\frac{\omega_o - \omega_1}{\omega_1} = 0.056$$

The above value is based on assumptions stated above. Eventually a better calculation of the synchronization condition must be made.

CHAPTER 4

CONCLUSION

The Savonius rotor is one of the most efficient but there is a minor problem with this design. The top bearing does not make constant contact with the top mount where the lead is connected, so the output wave form becomes a very noisy sine wave. We developed a top mount that has a spring from an old relay which adjusts its contact with the bearing at all times. This improved the signal modestly. It is possible to develop an improved bearing design so the contact becomes permanent.

The lateral leaf rotor is efficient also, but its tip speed ratio is quite low compared to that of the Savonius rotor. An intermediate size of lateral leaf rotor could be practical if it can be synchronized directly to the line. The calculation of synchronization for this generator limits the values of Q and ω_r such that they have to be fairly high for its operation.

The goal of improvement of the oscillating leaf generator is of major importance. This is because this

new generator oscillates at frequencies from 25 to 55 Hz with (tip speed)/(wind speed) ratios from 0.7 to 2. To get 60 Hz oscillation synchronized with the ac line, it is desirable to maximize the mechanical Q of the oscillation and the electromechanical coupling constant k^2 . The measured values of Q are in the 13 to 15 range, and improvements in Q are both possible and desirable.

To increase Q of the bimorph one has to explore the following alternatives:

1. Blade shape design.
2. Gluing technique if inert layer is different from PVF_2 .
3. New calculation for a better geometry of blade.
4. A better vortex maker to increase the amplitude of oscillation.

Operation as a line-independent generator in remote locations may be the first cost-effective application of this device. But testing of PVF_2 bimorphs under extreme temperature and wind conditions has not yet been done.

A major advantage of the PVF_2 wind generator is its compactness. Since the PVF_2 will create the power, there is no need for gear boxes or separate generators. The present cost of a 100 cm^2 piece of 110 micron thick uniaxial "Kynar" PVF_2 film is \$75.00 and the cost is almost proportional to its thickness. Using the value of

0.212 watts/cm³ power output computed in the energy analysis section in Appendix III, this becomes \$321 per watt. This is 200 times as expensive as the \$1.60/watt DOE goal for solar cell cost in 1985. The poled PVF₂ is very expensive, almost three times the price of gold. Clearly what is needed to be done is a breakthrough in the poling process which makes the polymer piezoelectric. In the meantime it seems wise to spend a very modest amount of money to develop the piezoelectric wind generator concept so it will be ready when the prices of PVF₂ polymer drop sharply. These design computations and preliminary wind tunnel tests show that a combination of better piezoelectric properties and lower cost are needed before these PVF₂ wind generators will be economically practical.

REFERENCES

REFERENCES

- Bikales, N.M. Mechanical Properties of Polymers, John Wiley and Sons New York, 1971.
- Cady, W.G. Piezoelectricity, McGraw-Hill Book Company, Inc., 1946.
- Kawai, H. Jpn. J. Appl. Phys. 8, 975, 1969.
- Keyser, Materials Science in Engineering, 3rd Ed., Charles E. Merrill Publishing Company, 1974.
- Lovinger, A.J., Science 220, 4602, 1983.
- Park, J. The Wind Power Book, Cheshire Books, Palo Alto, California, 1981.
- Schmidt, V.H., Klakken, M., and Darejeh, H. Experimental Study and Electromechanical Analysis of Oscillation of Piezoelectric Polymer Bimorphs as Wind Generator Elements, to appear in Proceedings of Wind Workshop VI (Minneapolis, June 1983).
- Schmidt, V.H. Proceedings of the 1981 Wind and Solar Energy Technology Conference (University of Missouri-Columbia Press), p. 97.
- Yoler, Y.A. A Study of Piezoelectric Elements for the Measurement of Transient Forces, United States Department of Commerce Office of Technical Services, PB 111702, February 1, 1955.

APPENDICES

APPENDIX I

Measurements, equipment diagrams and test plots.

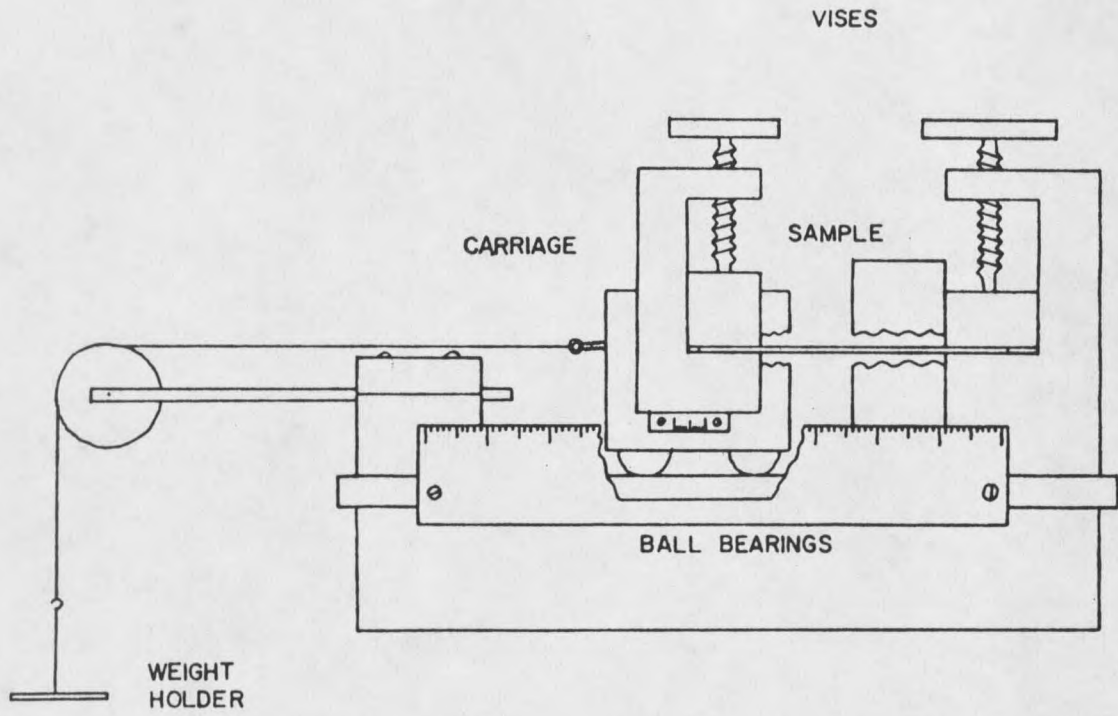


Figure 28. Y and d_{ij} measurement apparatus.

$$Y_{3m} = 1.4 \times 10^9 \frac{N}{m^2}$$

Yield strength at 0.3%

$$\text{Slope} = 1.633 \times 10^8 \frac{kg}{m^2}$$

$$Y = 1.6 \times 10^9 \frac{N}{m^2}$$

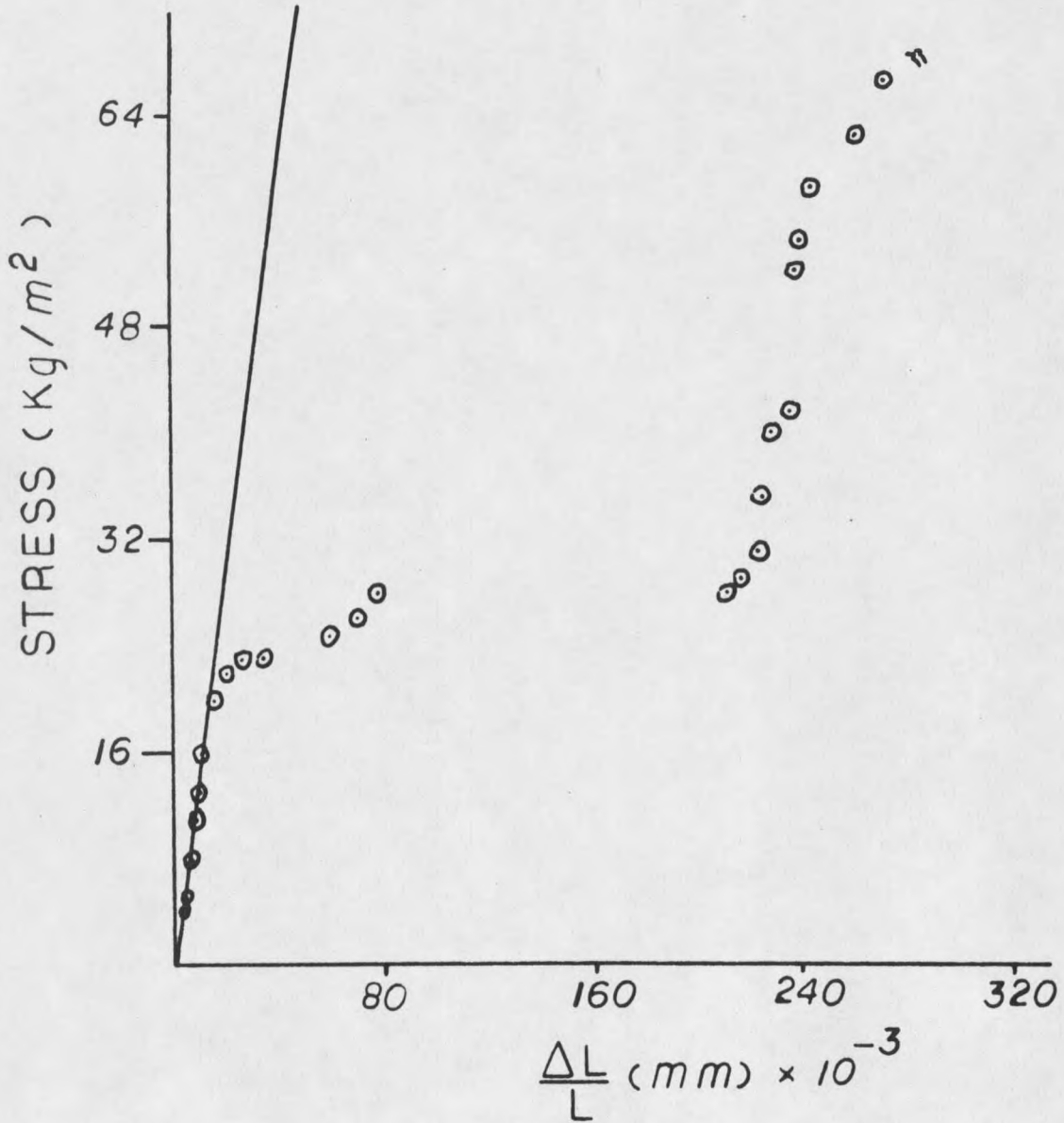


Figure 29. Stress-strain curve.

Size 1 by 2 cm
Thickness 30 micron

Slope $\sim 0.038 \frac{\text{mV}}{\text{gm}}$

$$d_{31} = 4 \times 10^{-12} \frac{\text{C}}{\text{N}}$$

Sample made by 3M

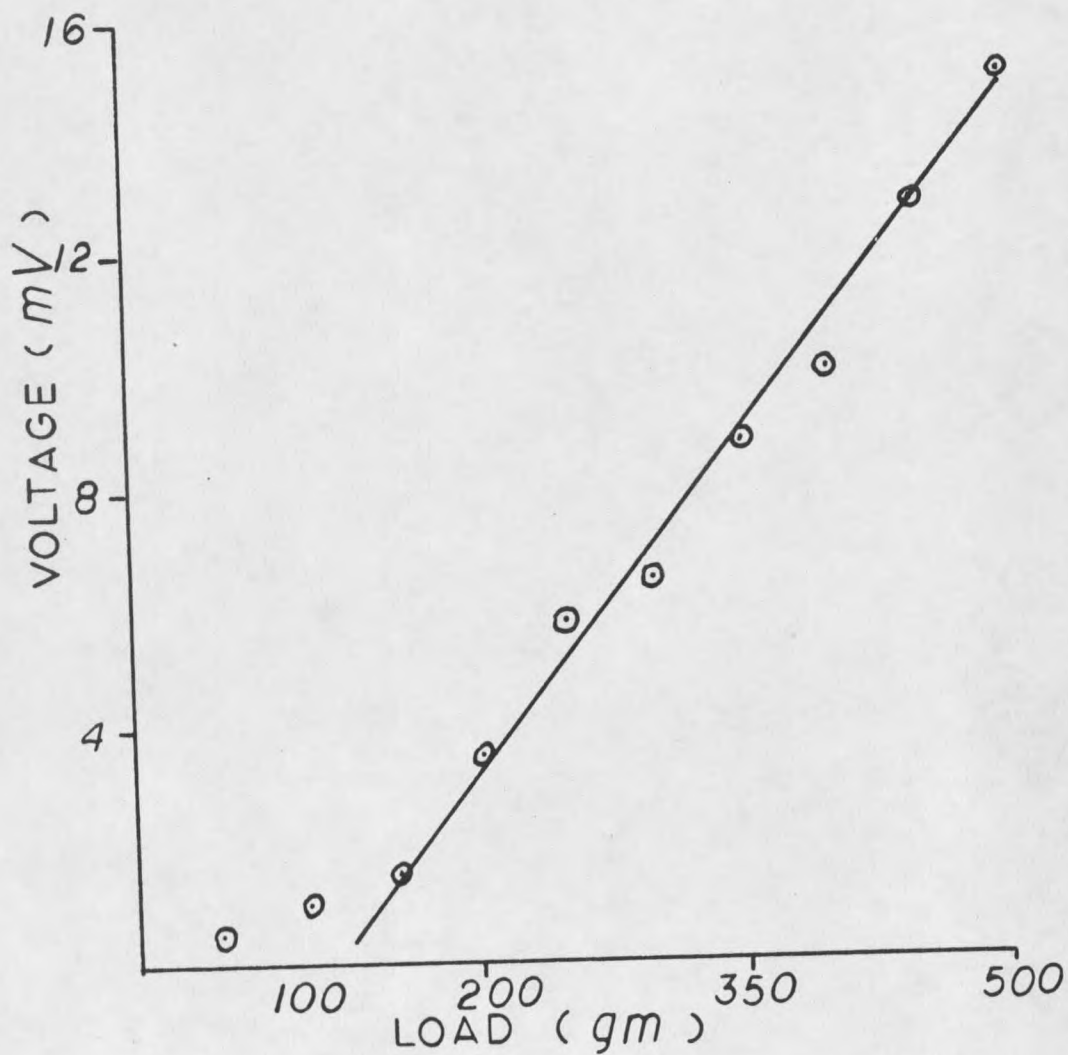


Figure 30. Load vs. voltage drop graph for d_{31}

Sample made by 3M
Size 1 by 2 cm
Thickness 30 micron
Slope ~ 0.0504
 $d_{32} = 5.36 \times 10^{-12} \frac{C}{N}$

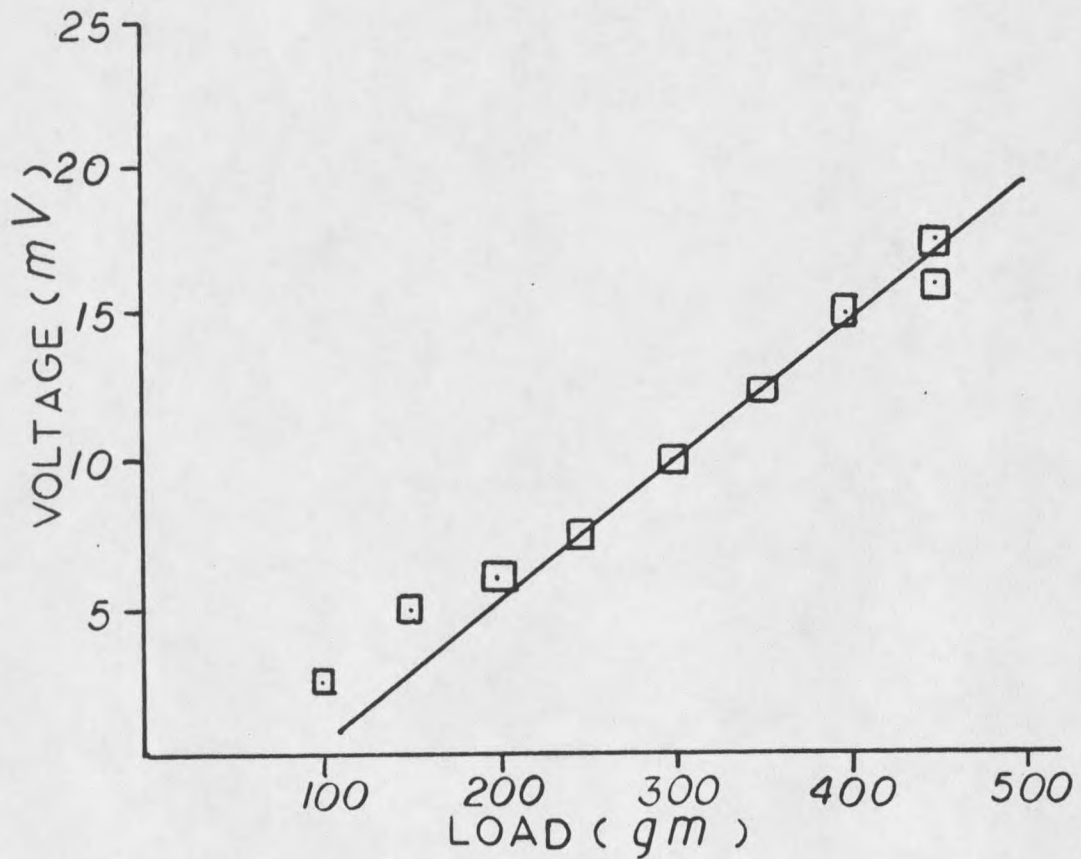


Figure 31. Load vs. voltage drop graph for d_{32}

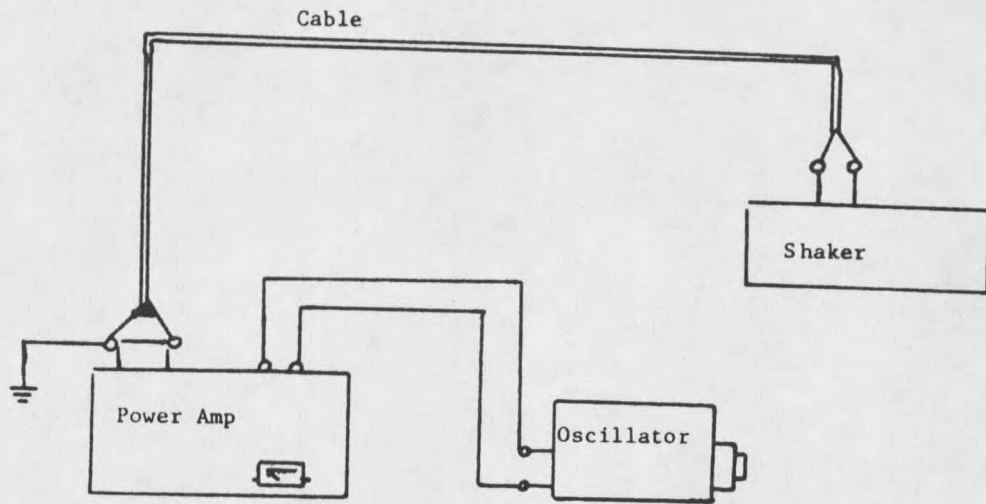


Figure 32. Circuit diagram for determining Q and f_r .

Shape : Tree leaf
 Width = 13.5 cm
 Height = 4.5 cm
 Blade thickness = 350 micron

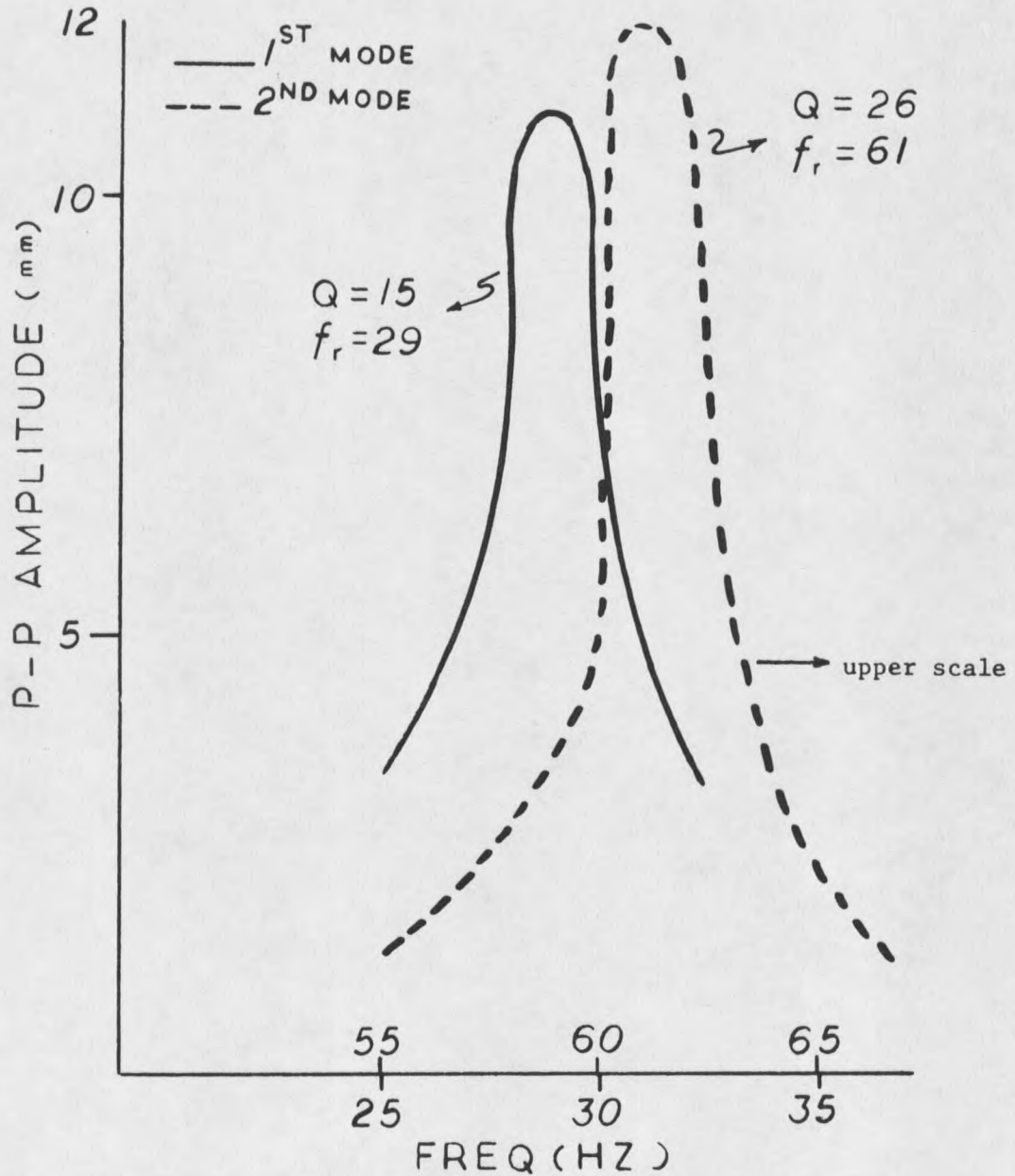


Figure 33. Plot of frequency vs. amplitude for Q and f_r determination.

APPENDIX II

Construction figures of lateral leaf rotor, design
parameter plot of α and power data.

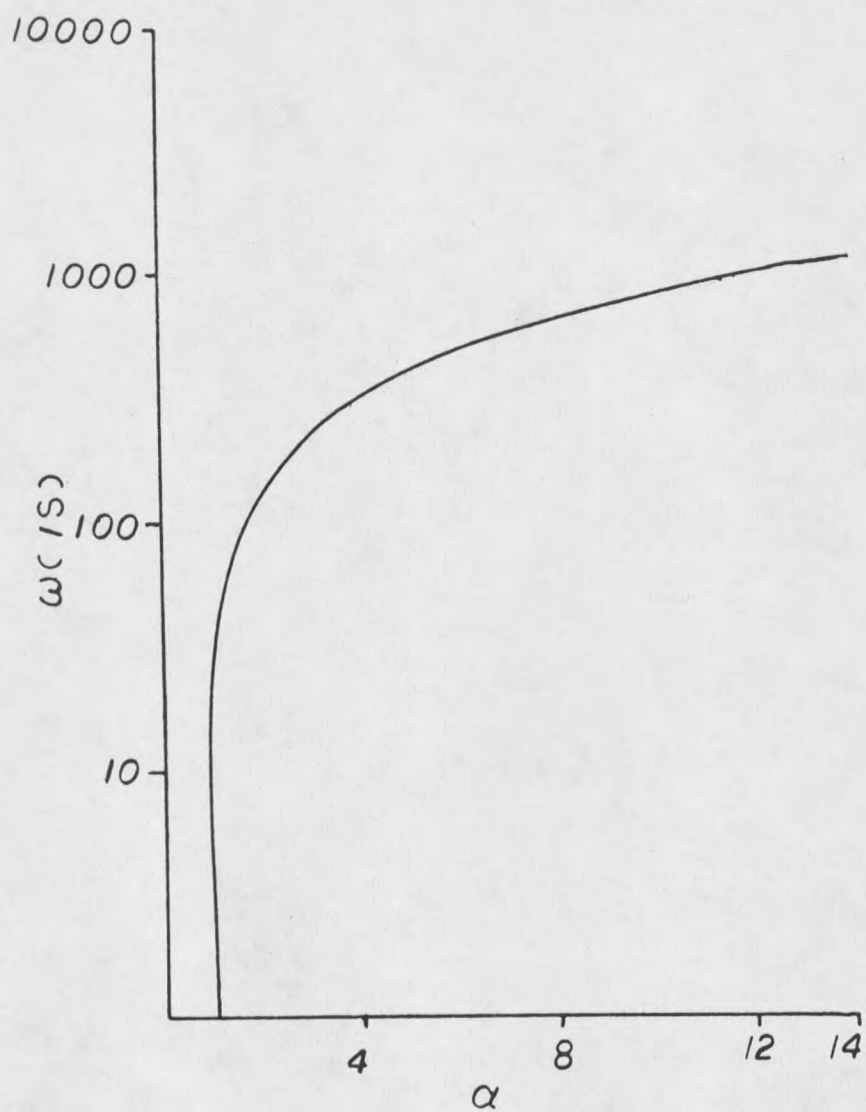


Figure 34. Plot of α vs. ω . Also see Procedure Section for $\alpha(\omega)$

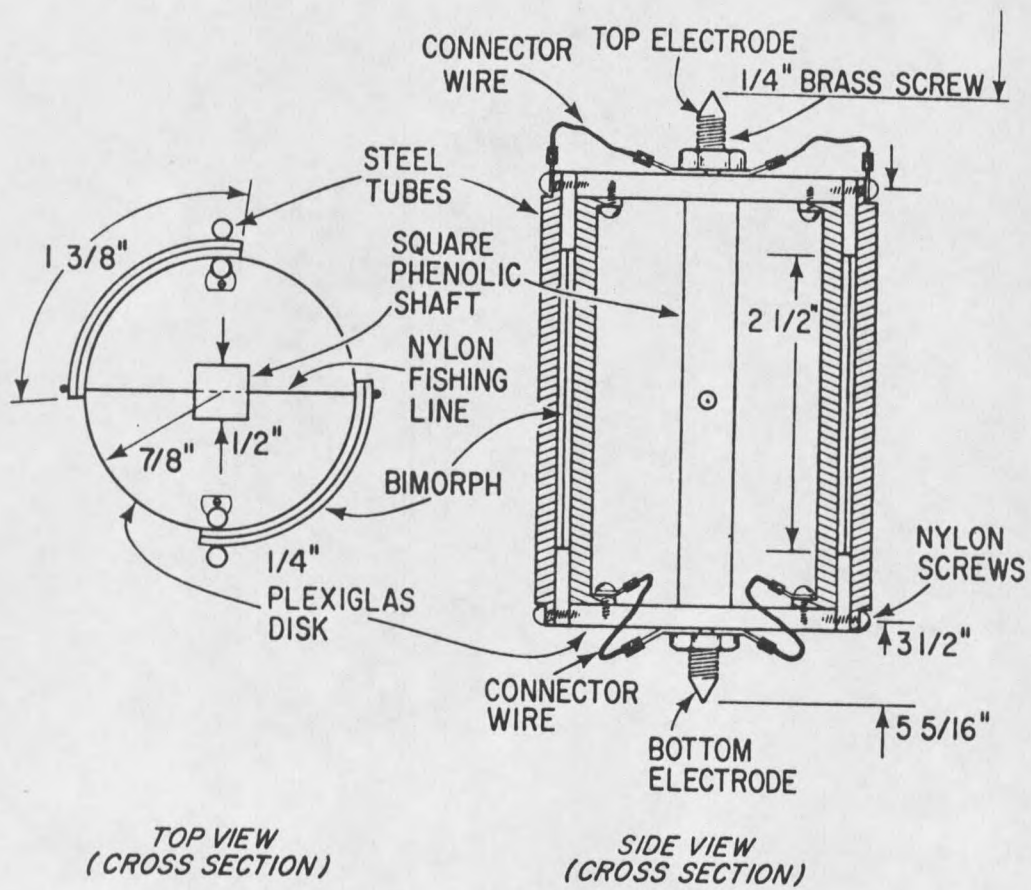


Figure 35. Lateral leaf rotor construction figure.

Power Data for Lateral Leaf Rotor

Wind Velocity V_w (m/s)	RPM	Tip Velocity (m/s)	Voltage (P-P) (V)	Load R(Ω)	Power (μ W)
9.6	750	2.1	5	100K	31.3
9.6	750	2.1	12	150K	120
9.6	750	2.1	17	220K	164
9.6	750	2.1	25	330K	237
9.6	750	2.1	30	470K	240
9.6	750	2.1	35	680K	225
9.6	750	2.1	40	1M	200
9.6	750	2.1	42	1.5M	147
9.6	750	2.1	44	2.2M	110
9.6	750	2.1	50	3.3M	126
9.6	750	2.1	45	5.7M	79
9.6	750	2.1	45	6.8M	62
9.6	750	2.1	45	10M	50
11.6	770	2.14	15	100K	281
11.6	770	2.14	20	150K	333
11.6	770	2.14	25	220K	355
11.6	770	2.14	30	330K	341
11.6	770	2.14	35	470K	326
11.6	770	2.14	43	680K	340
11.6	770	2.14	52	1M	338
11.6	770	2.14	55	1.5M	289
11.6	770	2.14	60	2.2M	250
11.6	770	2.14	65	3.3M	212.8
11.6	770	2.14	60	4.7M	150.3
11.6	770	2.14	60	6.8M	111
11.6	770	2.14	60	10M	90
15.7	770	2.14	25	150K	521
15.7	770	2.14	30	220K	511
15.7	770	2.14	35	330K	464
15.7	770	2.14	40	470K	425
15.7	770	2.14	60	1M	450
15.7	770	2.14	70	2.2M	339
15.7	770	2.14	65	4.7M	165
15.7	770	2.14	65	6.8M	130
15.7	770	2.14	65	10M	105.6

Wind Velocity V_w (m/s)	RPM	Tip Velocity (m/s)	Voltage (P-P) (V)	Load $R(\Omega)$	Power (μW)
22	920	2.55	30	150K	750
22	920	2.55	35	220K	696
22	920	2.55	40	330K	606
22	920	2.55	55	1M	587
22	920	2.55	60	2.2M	250
22	920	2.55	65	4.7M	165
22	920	2.55	60	6.8M	
22	920	2.55	60	10M	

Power Data for Oscillating Leaf

Wind Velocity (m/s)	Freq. (Hz)	Voltage (P-P) (V)	Load R(Ω)	Power (μ W)
1.6	25	1	150K	0.83
1.6	25	1.5	220K	1.28
1.6	25	2.3	330K	2
1.6	25	3	470K	2.4
1.6	25	4	680K	2.9
1.6	25	5.5	0.91M	4.2
1.6	25	8	1.3M	6.1
1.6	25	10	1.8M	6.9
1.6	25	12	2.5M	7.2
1.6	25	15	3.2M	8.9
1.6	25	17.5	4.55M	9.4
1.6	25	17.5	5M	8
2.85	25	1.3	150K	1.4
2.85	25	1.7	220K	1.6
2.85	25	2.4	330K	2.2
2.85	25	3.5	470K	3.3
2.85	25	4.5	680K	3.7
2.85	25	6	0.91M	4.95
2.85	25	8	1.3M	6.2
2.85	25	11	1.8M	8.4
2.85	25	13	2.5M	8.5
2.85	25	16	3.2M	10
2.85	25	17.5	4.55M	9.5
2.85	25	19	5M	9
7.1	25	2	150K	3.3
7.1	25	2.4	220K	3.3
7.1	25	3	330K	3.4
7.1	25	4	470K	4.3
7.1	25	5	680K	4.6
7.1	25	6	0.91M	4.95
7.1	25	8	1.3M	6.2
7.1	25	11	1.8M	8.4
7.1	25	13	2.5M	8.5
7.1	25	15	3.2M	8.8
7.1	25	17	4.55M	8.9
7.1	25	18	5M	8.1

APPENDIX III

Energy analysis calculation.

Energy Analysis

$$\delta = \frac{S}{Y} = 0.0294$$

$$R_{\min} = t/\delta_{\max} = 3.33 \text{ mm}$$

for $t = 100$ micron

$$T_o = 2Ywt^3/3R_{\min}$$

$$T_o = 8 \times 10^{-4} \text{ N-m}$$

Blade impedance $Z = -j/\omega c$

where, $\omega = 2\pi f = 2\pi(60)$

$$C = \epsilon_o \epsilon_r WL/2t$$

$$\epsilon_o = \text{Constant}$$

$$\epsilon_r = 12$$

$$W = 10 \text{ cm}$$

$$L = 0.52 \text{ cm}$$

then $|Z| = 9.61 \times 10^6$ ohms

$$V_o = 920 \text{ volts}$$

$$\text{output power} = \frac{1}{4} V_o^2 \omega c$$

$$\text{PVF}_2 \text{ Volume} = 10 \text{ cm} \times 0.52 \text{ cm} \times 0.02 \text{ cm}$$

$$\text{Power/Volume} = 0.212 \text{ W/cm}^3$$

The output power is 0.022 watts for a blade of 5.2×10^4 PVF₂ area facing the wind, but only 45% of the blade area is composed of PVF₂. Accordingly if a system of one square meter area facing the wind is packed densely with such blades, the output power would be 19.1 watts. This is fairly good compared with 100 watts/m² available from large conventional wind generators at design wind speed.

MONTANA STATE UNIVERSITY LIBRARIES
stks N378.D245@Theses RL
Piezoelectric polymer wind generators /



3 1762 00184023 8

N378
D245
cop. 2